

## Accepted Manuscript

Oxadiazolone derivatives, new promising multi-target inhibitors against *M. tuberculosis*

Phuong Chi Nguyen, Vincent Delorme, Anaïs Bénarouche, Alexandre Guy, Valérie Landry, Stéphane Audebert, Matthieu Pophillat, Luc Camoin, Céline Crauste, Jean-Marie Galano, Thierry Durand, Priscille Brodin, Stéphane Canaan, Jean-François Cavalier

PII: S0045-2068(18)30722-3  
DOI: <https://doi.org/10.1016/j.bioorg.2018.08.025>  
Reference: YBIOO 2482

To appear in: *Bioorganic Chemistry*

Received Date: 16 July 2018  
Revised Date: 17 August 2018  
Accepted Date: 20 August 2018

Please cite this article as: P. Chi Nguyen, V. Delorme, A. Bénarouche, A. Guy, V. Landry, S. Audebert, M. Pophillat, L. Camoin, C. Crauste, J-M. Galano, T. Durand, P. Brodin, S. Canaan, J-F. Cavalier, Oxadiazolone derivatives, new promising multi-target inhibitors against *M. tuberculosis*, *Bioorganic Chemistry* (2018), doi: <https://doi.org/10.1016/j.bioorg.2018.08.025>

This is a PDF file of an unedited manuscript that has been accepted for publication. As a service to our customers we are providing this early version of the manuscript. The manuscript will undergo copyediting, typesetting, and review of the resulting proof before it is published in its final form. Please note that during the production process errors may be discovered which could affect the content, and all legal disclaimers that apply to the journal pertain.



**Oxadiazolone derivatives, new promising multi-target inhibitors against *M. tuberculosis***

Phuong Chi Nguyen<sup>1§</sup>, Vincent Delorme<sup>2§#</sup>, Anaïs Bénarouche<sup>1</sup>, Alexandre Guy<sup>3</sup>, Valérie Landry<sup>2</sup>, Stéphane Audebert<sup>4</sup>, Matthieu Pophillat<sup>4</sup>, Luc Camoin<sup>4</sup>, Céline Crauste<sup>3</sup>, Jean-Marie Galano<sup>3</sup>, Thierry Durand<sup>3</sup>, Priscille Brodin<sup>2</sup>, Stéphane Canaan<sup>1\*</sup> and Jean-François Cavalier<sup>1\*</sup>

<sup>1</sup> Aix-Marseille Univ, CNRS, LISM, Institut de Microbiologie de la Méditerranée, Marseille, France

<sup>2</sup> Univ. Lille, CNRS, INSERM, CHU Lille, Institut Pasteur de Lille, U1019 - UMR 8204 - CIIL - Center for Infection and Immunity of Lille, Lille, France

<sup>3</sup> Institut des Biomolécules Max Mousseron (IBMM), UMR 5247, Université de Montpellier, CNRS, ENSCM, 15 Avenue Charles Flahault, 34093 Montpellier Cedex 5, France

<sup>4</sup> Aix-Marseille Univ, Inserm, CNRS, Institut Paoli-Calmettes, CRCM, Marseille Protéomique, Marseille, France

§ Authors have contributed equally to this work

Corresponding authors: [jfcavalier@imm.cnrs.fr](mailto:jfcavalier@imm.cnrs.fr) (J.-F. Cavalier); [canaan@imm.cnrs.fr](mailto:canaan@imm.cnrs.fr) (S. Canaan)

# Current Address: Tuberculosis Research Laboratory, Institut Pasteur Korea, Seongnam-si, Gyeonggi-do, 13488 Republic of Korea.

## ABSTRACT

A set of 19 oxadiazolone (**OX**) derivatives have been investigated for their antimycobacterial activity against two pathogenic slow-growing mycobacteria, *Mycobacterium marinum* and *Mycobacterium bovis* BCG, and the avirulent *Mycobacterium tuberculosis* (*M. tb*) mc<sup>2</sup>6230. The encouraging minimal inhibitory concentrations (MIC) values obtained prompted us to test them against virulent *M. tb* H37Rv growth either in broth medium or inside macrophages. The **OX** compounds displayed a diversity of action and were found to act either on extracellular *M. tb* growth only with moderated MIC<sub>50</sub>, or both intracellularly on infected macrophages as well as extracellularly on bacterial growth. Of interest, all **OX** derivatives exhibited very low toxicity towards host macrophages. Among the six potential **OXs** identified, **HPOX**, a selective inhibitor of extracellular *M. tb* growth, was selected and further used in a competitive labelling/enrichment assay against the activity-based probe Desthiobiotin-FP, in order to identify its putative target(s). This approach, combined with mass spectrometry, identified 18 potential candidates, all being serine or cysteine enzymes involved in *M. tb* lipid metabolism and/or in cell wall biosynthesis. Among them, Ag85A, CaeA, TesA, KasA and MetA have been reported as essential for *in vitro* growth of *M. tb* and/or its survival and persistence inside macrophages. Overall, our findings support the assumption that **OX** derivatives may represent a novel class of multi-target inhibitors leading to the arrest of *M. tb* growth through a cumulative inhibition of a large number of Ser- and Cys-containing enzymes involved in various important physiological processes.

## Keywords

Tuberculosis, Oxadiazolone, Lipolytic enzyme inhibitors, Activity-based probe (ABP)

## Abbreviations

ABPP, activity-based protein profiling; CC<sub>50</sub>, compound concentration leading to 50% of cell cytotoxicity; CyC, Cyclopostins & Cyclophostin analogs; ETO, ethionamide; FM, foamy macrophages; HSL, hormone-sensitive lipase; ILI, intracytoplasmic lipid inclusions; INH, isoniazid; MDR, multidrug-resistant strains; MIC<sub>50</sub>, minimal inhibitory concentration leading to 50% of growth inhibition; *M. tb*, *Mycobacterium tuberculosis*; pNP, *para*-nitrophenyl; REMA, resazurin microtiter assay; RIF, rifampicin; TB, tuberculosis; TAG, triacylglycerols; TDR, totally drug-resistant strains; XDR, extensively drug-resistant strains;  $x_i$ , inhibitor molar excess related to 1 mol of enzyme;  $x_{150}$ , inhibitor molar excess leading to 50% enzyme inhibition.

## 1. Introduction

With 10.4 million new cases and 1.7 million deaths in 2016, tuberculosis (TB) caused by the pathogenic species *Mycobacterium tuberculosis* (*M. tb*) remains the leading cause of death worldwide from a single infectious agent [1]. Despite the quadritherapy treatment involving isoniazid (INH), pyrazinamide, rifampicin (RIF) and ethambutol, the introduction of new molecules on the market to strengthen or replace this first-line antibiotics regimen is a slow and tedious process [2, 3]. Only a few drugs were able to pass the selection stages (*e.g.*, bedaquiline [4], delamanid [5] and PA-824 [6]). However, the appearance and spread of multidrug-resistant (MDR), extensively drug-resistant (XDR) and totally drug-resistant (TDR) strains [7-10] highlights the urgent need for finding new therapeutic options to fight against *M. tb*.

In this context, oxadiazolone-core (**OX**) compounds represent attractive tools. Compound **S57** (**Figure 1A**), initially described in 1954 [11, 12] as being active against TB [13-15], was used as template for the synthesis of 3,5-substituted 1,3,4-oxadiazole-2-one derivatives [16, 17]. These molecules were found to exhibit interesting anti-mycobacterial activity against *M. tb* H37Rv, with minimal inhibitory concentrations (MIC) of 1.25–8 µg/mL, comparable to those of INH (0.5 µg/mL) and RIF (1.0 µg/mL) [16, 17]. Molecular modeling indicated that these compounds possessed all necessary features to block the enzymatic activity of the mycobacterial cytochrome P450-dependent 14 $\alpha$ -sterol demethylase (P450<sub>14DMs</sub>) [18], also a target for antifungal drug design [19]. These findings thus suggest the potential use of such **OX** derivatives as alternative therapeutic agents for TB [20].

Few years ago, we reported that the **OX** compound **MmPPOX** (**Figure 1B**), a reversible inhibitor of the hormone-sensitive lipase (HSL) family of proteins [21, 22], was able to inhibit the growth of *M. tb* with MIC values of around 15-25 µg/mL as determined on solid medium [23]. Keeping in mind its strong affinity toward the HSL family member proteins (Lip-HSL), we further investigated the *in vitro* inhibition of recombinant *M. tb* Lip-HSL. As expected, the nine purified Lip-HSL enzymes tested were all strongly inhibited by **MmPPOX**, which reacted with the catalytic serine

residue by forming a covalent but (slowly) reversible bond (*i.e.*, carbamate or thiocarbamate bond, **Figure 1B**). Such an inhibitor could then be considered as a long-life substrate rather than a true inhibitor as already observed with Orlistat (also named Tetrahydrolipstatine or THL), a representative member of reversible serine hydrolase inhibitors [24-26].

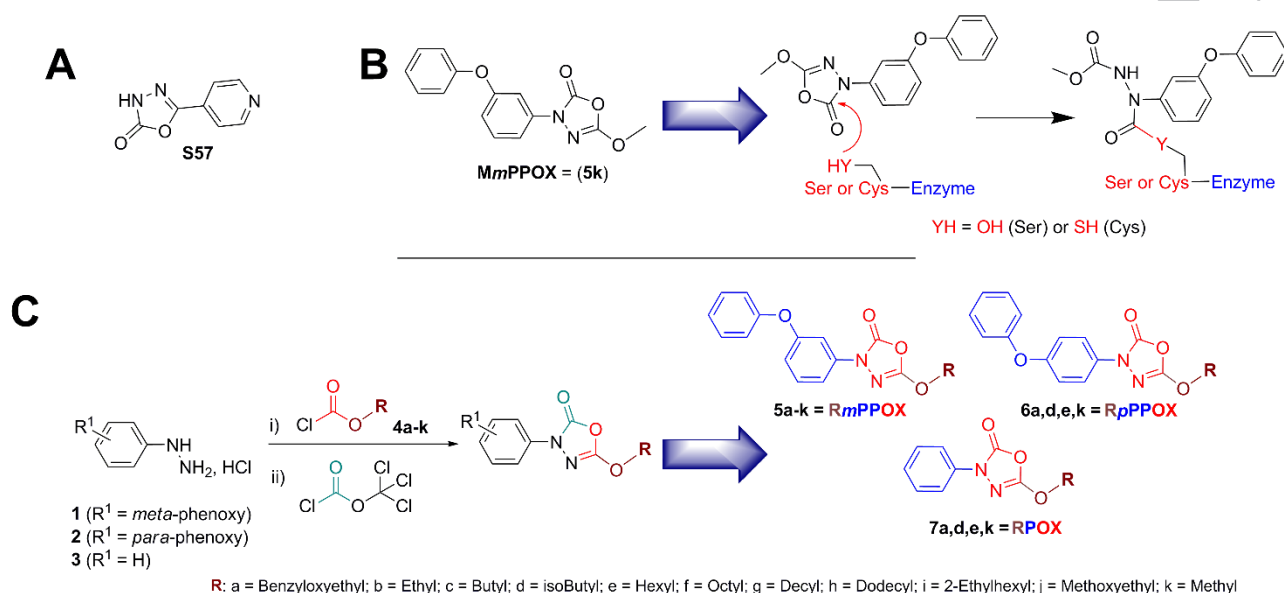


**Figure 1.** Chemical structure of (A) 5-(pyridin-4-yl)-1,3,4-oxadiazol-2(3*H*)-one **S57**, and (B) 5-methoxy-3-(3-phenoxyphenyl)-1,3,4-oxadiazol-2(3*H*)-one **MmPPOX** and its mode of action. (C) General procedure for the one step preparation of 5-alkoxy-3-phenyl substituted-1,3,4-oxadiazol-2(3*H*)-one compounds from either (3-phenoxyphenyl)hydrazine hydrochloride (**1**), (4-phenoxyphenyl)hydrazine hydrochloride (**2**) or phenylhydrazine hydrochloride (**3**), giving **OX** derivatives **5a-k** (*i.e.*, **RmPPOX**), **6a,d,e,k** (*i.e.*, **RpPPOX**) or **7a,d,e,k** (*i.e.*, **RPOX**), respectively. Reagents and conditions: i) Alkyl chloroformate **4a-k**, Pyridine, 0 °C to RT; ii)  $ClCO_2CCl_3$ ,  $CHCl_2$ , Pyridine, 0 °C to RT, 40-85%. Adapted from [27].

From these first results, a new series of 18 lipophilic **OX** derivatives based on **MmPPOX** core-structure have been synthesized (**Figure 1C**) and tested for their anti-mycobacterial activities. More precisely, each oxadiazolone molecule has been tested against *M. tb* H37Rv for *i*) its capacity to inhibit *in vitro* growth; *ii*) its antitubercular activity on *M. tb*-infected macrophages, and *iii*) its cytotoxicity towards macrophages. Interestingly, some analogs were found to inhibit *M. tb* growth *in vitro* and/or inside macrophages without any significant toxicity to host cells. In addition, using

an activity-based protein profiling (ABPP) assay, the potential target enzymes of **HPOX**, acting only on *M. tb* extracellular growth, were further identified.

ACCEPTED MANUSCRIPT

## 2. Results and Discussion

### 2.1 Synthesis of oxadiazolone-core (OX) derivatives.

The set of new 18 lipophilic **OX** derivatives based on **MmPPOX** core-structure was designed by varying the nature of the **R** chain and/or the positioning of the phenoxy group (in *meta* or *para* position) when present (**Figure 1C**), and synthesized as previously reported [27]. The (phenoxy)phenyl group, proposed to be responsible for strong hydrophobic interactions and structural stiffening [27], was conserved in most of the new candidate inhibitors. In addition, modifying the **R** chain born by the oxadiazolone ring allow an investigation of the influence of the lipophilicity on the antibacterial activity exerted by these molecules. To remain consistent with previous studies involving such compounds [23, 27], we have decided to use the specific nomenclature already developed for these derivatives noted **Rm(or p)PPOX**; where **m(or p)P** represents the *meta* (or *para*)-Phenoxy group when present; **P** the phenyl group; **OX** the Oxadiazolone core; and **R** the alkyl chain (*i.e.*, Be, benzyloxyethyl; M; methyl, E, ethyl; B, butyl; iB, isobutyl; H, hexyl; O, octyl; Eh, 2-ethylhexyl; D, decyl; Do, dodecyl; Me, methoxyethyl).

### 2.2 Susceptibility testing on selected mycobacteria.

The antibacterial properties of the **OX** compounds were first evaluated towards three slow-growing mycobacteria: *M. marinum*, *M. bovis* BCG and *M. tb* mc<sup>2</sup>6230, a H37Rv strain with its RD1 region and *panCD* genes deleted, resulting in an avirulent pan(-) phenotype [28]. The corresponding MIC<sub>50</sub> values, as determined by the REMA assay [29-32], are reported in **Table 1**. First, it is noteworthy that the concentrations needed to inhibit 50% of the bacterial growth (MIC<sub>50</sub>) obtained for rifampicin (RIF) and isoniazid (INH), used here as reference antibiotics, were in agreement with literature data [33-35].

Nearly all 19 **OXs** were active against *M. bovis* BCG and *M. marinum* growth (**Table 1**). However, with MIC<sub>50</sub> values in the range 1.9-53 µM, *M. marinum* was nearly 2-times more sensitive to **OX** compounds than *M. bovis* BCG (MIC<sub>50</sub> from 3.5 to >120 µM). **BePOX**, **HPOX** and **iBPOX**, for

which the phenoxy substituent is absent, exhibited the most potent antibacterial activity towards *M. marinum*, with mean MIC<sub>50</sub> of 2.3 ± 0.33 μM, comparable to that of RIF (1.4 μM). Interestingly, these three **OX** compounds were also among the best inhibitors of *M. bovis* BCG growth; **HPOX** being the best one (MIC<sub>50</sub> = 3.5 μM).

From these encouraging data obtained using two slow-growing mycobacteria, it was tempting to extrapolate that these **OXs** would behave in a similar way against *M. tb* growth and conclude that the same three compounds, *i.e.* **BePOX**, **HPOX** and **iBPOX**, would then be promising anti-TB molecules.

Drug susceptibility testing of the 19 **OXs** was thus further assessed using the non-virulent *M. tb* mc<sup>2</sup>6230 strain. Among all tested compounds, 14 **OXs** were active against *M. tb* mc<sup>2</sup>6230. The two best growth inhibitors obtained were **iBpPPOX** and **BePOX**, which displayed similar MIC<sub>50</sub> value (mean 32.1 ± 1.0 μM). In all other cases, MIC<sub>50</sub> values were indicative either of a weak (mean MIC<sub>50</sub> = 84.1 ± 9.1 μM for **MmPPOX**, **MPOX** and **MemPPOX**), or a moderate (mean MIC<sub>50</sub> = 46.9 ± 5.1 μM for **BmPPOX**, **iBmPPOX**, **HmPPOX**, **HpPPOX**, **HPOX**, **OmPPOX**, **EhmPPOX**, **BemPPOX** and **BepPPOX**) antibacterial activity (Table 1). From these data, *M. tb* mc<sup>2</sup>6230 was found nearly 13- and 5-times less sensitive to the **OX** compounds than *M. marinum* and *M. bovis* BCG, respectively.

Surprisingly, **iBPOX**, which differs from **BePOX** and **HPOX** by the length of its **R** substituent, was not active against this mycobacteria. Moreover, no clear trends or rules in terms of structure-activity relationships (SAR) have emerged regarding the potency of these oxadiazolone-core compounds against *M. marinum* and *M. bovis* BCG. Indeed, increasing the lipophilicity by varying the nature of the **R** chain on the oxadiazolone ring and/or the positioning of the phenoxy group when present had no real impact on the anti-mycobacterial activity.

Interestingly, with *M. tb* mc<sup>2</sup>6230, some SAR tendencies can however be set up. First, and as mentioned above, the positioning of the phenoxy group in *meta* or *para* position has no real impact on the antibacterial activity of the corresponding compounds (*i.e.*, **MmPPOX** vs. **MpPPOX**;

**iBmPPOX** vs. **iBpPPOX**; **HmPPOX** vs. **HpPPOX**; **BemPPOX** vs. **BepPPOX**). Remarkably, **iBPOX** bearing the short chain isobutyl has no activity as compared to the phenoxyphenyl derivatives **iBpPPOX** and **iBmPPOX**. This is however not the case with the medium chains hexyl and benzyloxyethyl **OXs**, for which the respective activity of **HPOX** and **BePOX** is retained and even slightly better than **HmPPOX** & **HpPPOX** on the one hand, and **BemPPOX** & **BepPPOX** on the other hand. Finally, in absence of the bulky phenoxy group, the best MIC<sub>50s</sub> against *M. tb* mc<sup>2</sup>6230 were also obtained with **HPOX** and **BePOX** vs. **MPOX** and **iBPOX**. In brief, the **R** chain length thus seems to affect the potency of the tested compounds. More globally, the best growth inhibitors were found to carry a middle chain length of around 6 to 9 carbon atoms (*i.e.*, hexyl, 2-ethylhexyl, octyl or benzyloxyethyl chains). Longer or shorter chain's **OXs** (*i.e.*, methyl, methoxyethyl, ethyl, decyl or dodecyl) exhibited no or only very poor activity.

In summary, **iBpPPOX** displayed the best, while still moderate, antibacterial activity against *M. tb* mc<sup>2</sup>6230. The reason why such differences exist between the activity of the **OX** compounds against *M. marinum* and *M. bovis* BCG, compared to *M. tb*, is not clear and will need further studies to be elucidated; but differences in membrane composition and permeability are likely playing a role in this phenotype.

### 2.3 High-content screening assay on virulent *M. tb* H37Rv.

As recently observed for another class of potent *M. tb* growth inhibitors, the Cyclopiostins & Cyclophostin analogs (**CyC**) [31], MIC<sub>50</sub> values determined against *M. tb* mc<sup>2</sup>6230 do not necessarily correlate with the activity against *M. tb* H37Rv, particularly the activity against intracellular bacteria.

Consequently, each of the 19 **OX** derivatives have been further evaluated for their specific antitubercular activity against extracellularly- and intracellularly-growing virulent *M. tb* H37Rv-GFP strain, using a high-content screening assay based on the fluorescence measurement of GFP-expressing bacteria. *In vitro* growth (*i.e.*, extracellular assay) of *M. tb* H37Rv-GFP was first

monitored after 5 days at 37°C in presence of increasing concentrations of candidate inhibitors [31, 36-38]. Intracellular growth of *M. tb* H37Rv-GFP was also assessed following a 5-day exposure of infected Raw264.7 murine macrophage cell line to the various **OX** compounds. In this case, the percentage of infected cells, the total number of bacteria, the number of bacteria per infected cells, as well as the number of living host cells allowed us to determine the MIC<sub>50</sub> of the compound [36, 39, 40]. In subsequent experiment, the concentration leading to 50% of host cell cytotoxicity, *i.e.* CC<sub>50</sub>, were also determined in absence of infection.

Among all tested molecules, 6 potential **OX** candidates exhibited interesting antitubercular properties (**Table 2** and **Figure 2**). **BePOX** and **HPOX** impaired exclusively *M. tb* growth in culture broth medium with the same moderate MIC<sub>50</sub> (30.8 and 44.6 µM, respectively) than obtained previously on *M. tb* mc<sup>2</sup>6230. In contrast, **iBPOX**, **HpPPOX** and **BepPPOX** showed a clear preference against intracellularly-replicating mycobacteria with similar MIC<sub>50</sub> values (3.5-17.1 µM) than the first line antibiotics. Of interest, only **iBpPPOX** exhibited moderate (32.0 µM) to quite good (8.5 µM) activity against both extracellular and intramacrophagic *M. tb*, respectively (**Figure 2**).

Beside antibacterial activity, significantly, all these 6 **OX** inhibitors exhibited very low toxicity towards host macrophages with CC<sub>50</sub> > 100 µM, similarly to INH (CC<sub>50</sub> > 150 µM) and ethionamide (CC<sub>50</sub> ≥ 120 µM), two potent anti-TB drugs (**Table 2**). Their respective selectivity index (SI = CC<sub>50</sub>/MIC<sub>50</sub>) on intramacrophagic *M. tb* vs. Raw264.7 cells was thus found to be in a range from 5.8 and up to 28. While these are preliminary results that would need to be confirmed in other cell types including hepatocytes, they are encouraging for further improvement of the **OX** compounds. This absence of cytotoxicity was actually not obvious, given the number of (Ser/Cys)-enzymes present in host cells and the predicted potency of the **OX** compounds to target these classes of enzymes.

Interestingly, the observed differences in the behavior of **OX** compounds; in particular the higher activity against intracellular bacteria than against extracellular ones, have also been reported in the

case of the **CyC** compounds family [31]. As previously discussed above, inhibition of *M. tb* H37Rv may result from several (and probably different) mechanisms of action or penetration of the **OX** derivatives. With the hexyl and benzyloxyethyl chain, the absence/presence of the phenoxy group in *para* position clearly shifted the activity of the corresponding **OX** from extracellular- (*i.e.*, **HPOX** & **BePOX**) to intracellular-replicating bacilli (*i.e.*, **HpPPOX** & **BepPPOX**). On the other hand, with the short isobutyl chain, both **iBpPPOX** and **iBPOX** are found most active against intramacrophagic-replicating *M. tb*.

From these findings, it is tempting to assume that these **OX** compounds thus lead to the inhibition of specific but most likely distinct mycobacterial target enzymes between intramacrophagic- vs. extracellularly-replicating bacilli.

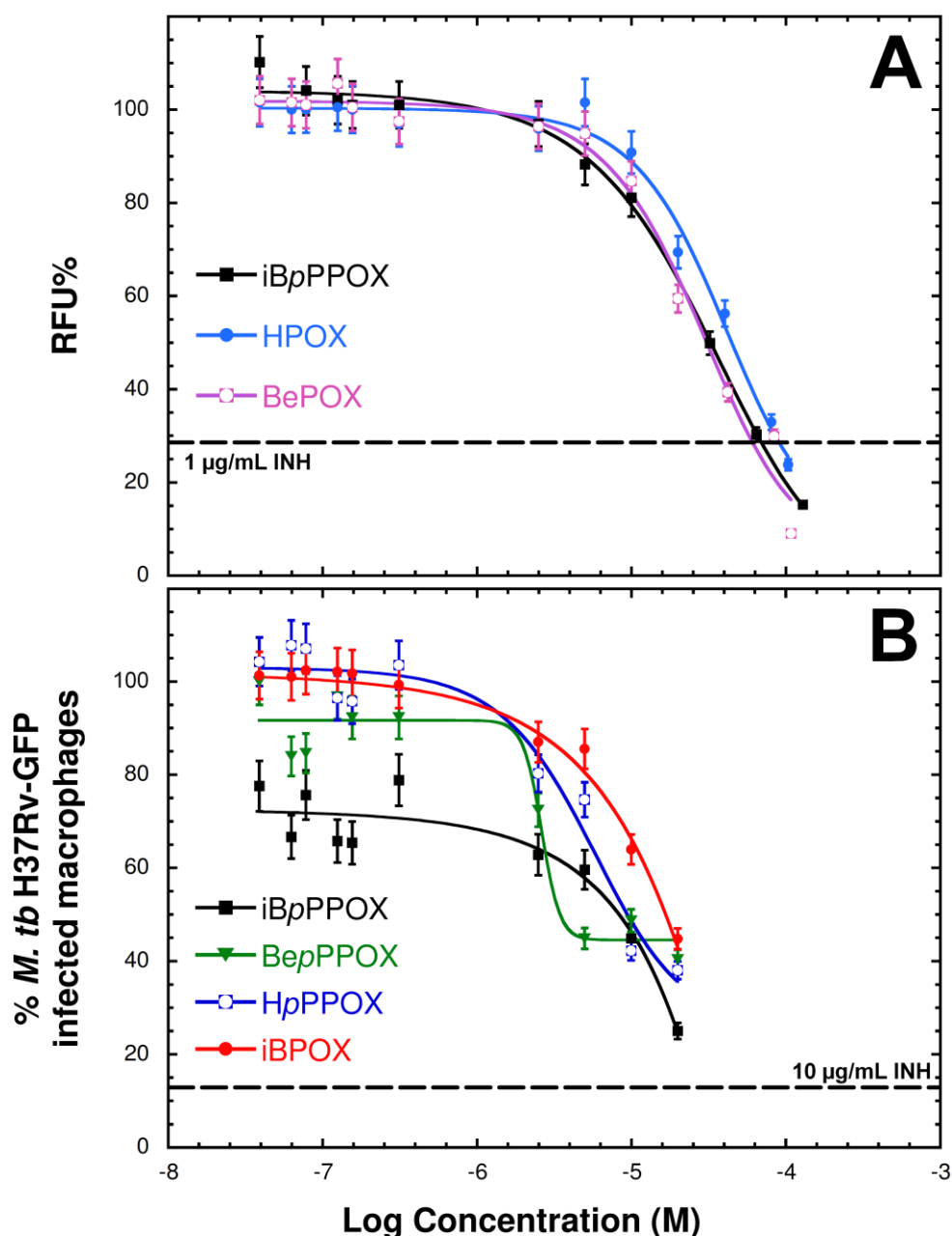


**Figure 2.** *In vitro* and *ex vivo* dose-response activity of the OX derivatives against *M. tb* H37Rv. (A) Activity of BePOX, iBpPPOX and HPOX against GFP-expressing *M. tb* replicating in broth medium, expressed as normalized relative fluorescence units (RFU%). The dashed line represents the level of inhibition (~70%) reached with 1 µg/mL (=7.3 µM) INH as control. The MIC<sub>50</sub> of BePOX, iBpPPOX and HPOX replicating in culture broth medium were 30.8 µM, 32.0 µM and 44.6 µM, respectively. (B) Activity of iBpPPOX, BepPPOX, HpPPOX and iBPOX against *M. tb* replicating inside Raw264.7 macrophages. Results are expressed as the percentage of infected macrophages after 5 days post-infection. The dashed line represents the level of inhibition (~87%) reached with 10 µg/mL (=73 µM) INH as control. The MIC<sub>50</sub> of BepPPOX, iBpPPOX, HpPPOX and iBPOX replicating inside macrophages were 3.5 µM, 8.5 µM, 9.5 µM and 17.1 µM, respectively. Each value is the mean ± SD for a triplicated dose-response. Experiments were conducted at least twice with consistent results.

#### 2.4 Targets identification by Activity-based protein profiling.

Based on the aforementioned results, and taking into account their strong affinity for Serine and/or Cysteine (Ser/Cys)-based enzymes (**Figure 1B**), one can hypothesize that **OX** inhibitors might target and impair the activity of various enzymes involved in several processes of *M. tb* pathogenic life cycle, thus resulting in bacterial death without any cytotoxicity towards host cells. Accordingly, target(s) identification experiments were conducted by applying an activity-based protein profiling (ABPP) approach [41-44]. In order to take into account the penetration/diffusion of the inhibitor through the mycobacterial cell wall, all experiments have been performed on living bacterial cells and not with a lysate, as previously described [31].

Here, **HPOX**, that selectively inhibits *M. tb* growth only in culture broth medium, was selected for such experiments. *M. tb* mc<sup>2</sup>6230 cells were grown to log phase and then incubated with **HPOX** compound or DMSO as a control. After cell lysis, part of the lysate was used for competitive probe labelling/enrichment assay using the Desthiobiotin-FP probe, targeting (Ser/Cys)-based enzymes [43] (**Figure 3**). In parallel, the remaining lysate was incubated with TAMRA-FP, also targeting (Ser/Cys)-based enzymes [43], to reveal the candidates presumably reacting with **HPOX** on SDS-PAGE gel, using fluorescence scanning [31]. Around 9 distinct bands labelled by TAMRA-FP were visible in the fluorescence readout (**Figure 3B –lane E**) and could also be detected by silver staining after release of the enzymes captured by Desthiobiotin-FP (**Figure 3B – lane B**). In contrast, pre-treatment with **HPOX** (**Figure 3A**) resulted in a decrease in fluorescence intensity of all visible bands, as exemplified by the black arrows in **Figure 3B – lane D**. Indeed, the enzymes previously inactivated by **HPOX** inhibitor will thus be unable to further react with the probes. The respective enriched mixtures (**Figure 3B – lanes A-B**) were digested with trypsin and the resulting peptides were analyzed by liquid chromatography-tandem mass spectrometry (LC-MS/MS) followed by subsequent label free quantification analysis. The proteins that were also found in the

control experiment (*i.e.*, **Figure 3B - lane A**: DMSO alone for unspecific binding to streptavidin-magnetic beads) were not taken into account.

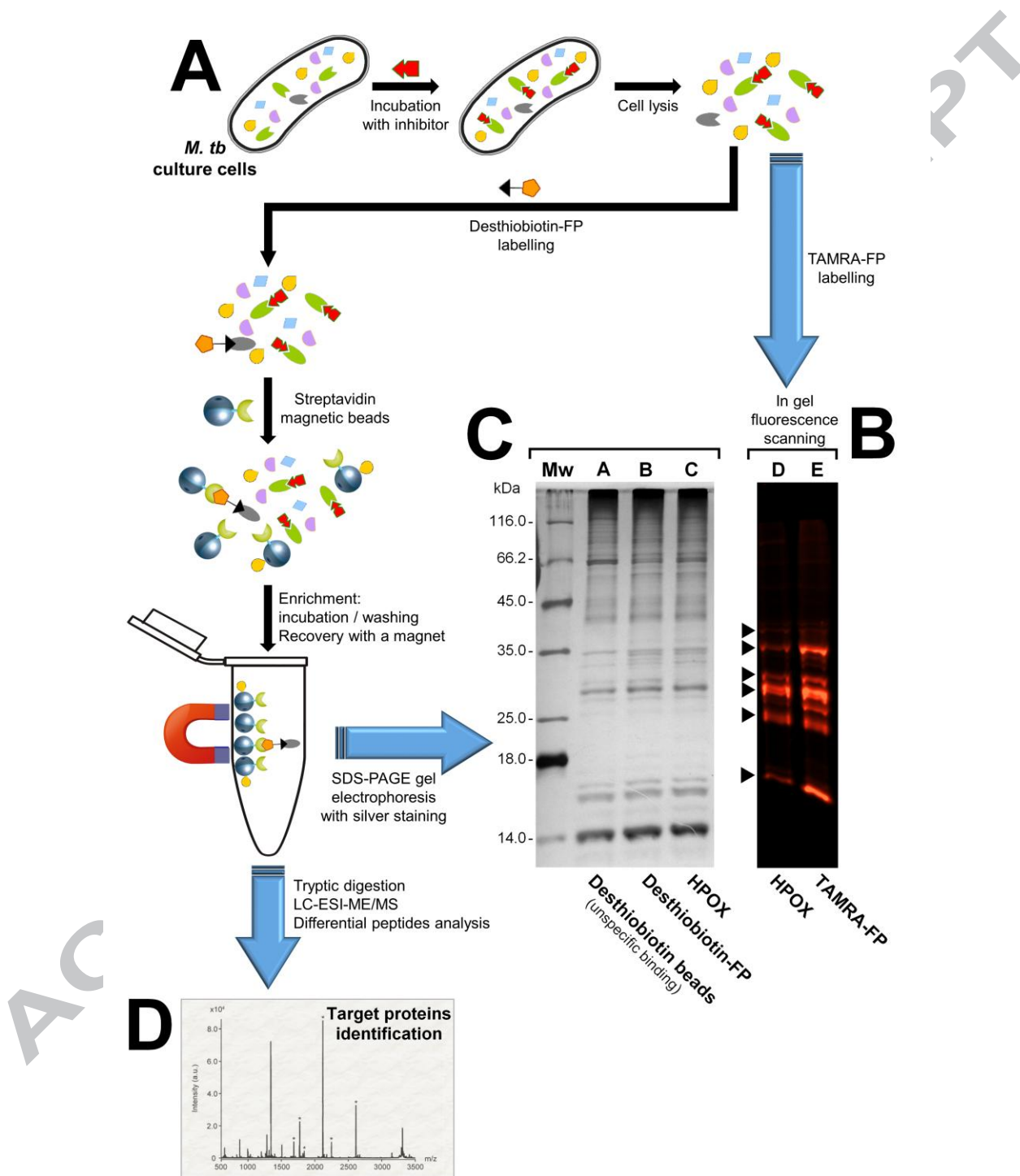


**Figure 3. Activity based protein profiling (ABPP) workflow for the identification of the proteins covalently bound to OX inhibitors.** (A) Cell culture of *M. tb* mc<sup>2</sup>6230 was pre-treated with selected HPOX inhibitor prior to cell lysis and further incubation with TAMRA-FP or Desthiobiotin-FP probe. In this latter case, samples were then treated with streptavidin-magnetic beads for the capture and enrichment of labelled proteins. (B-C) Equal amounts of proteins obtained in A were separated by SDS-PAGE and visualized by in-

gel fluorescence (*right* panel - lanes D-E: TAMRA detection) or silver staining (*left* panel – lanes A-C). Enzymes whose TAMRA-FP labelling is impeded because of the presence of **HPOX** in their active-site are shown by arrowheads. **(D)** Tryptic digestion followed by tandem mass spectrometry analyses and subsequent differential proteomics analysis allowed identifying the target proteins.

ACCEPTED MANUSCRIPT

The resulting mycobacterial targets of **HPOX** were displayed as volcano plot (**Figure 4**). Only proteins identified with a permutation false discovery rate (pFDR) of 5% and a score threshold value  $\geq 60$  were selected, therefore leading to a panel of 18 distinct proteins (**Table 3**). These identified enzyme candidates ranged in their functional category from intermediary metabolism/respiration (6 proteins), lipid metabolism (5 proteins), cell wall/cell processes (6 proteins), and virulence / detoxification / adaptation (1 protein) (**Table 3**).

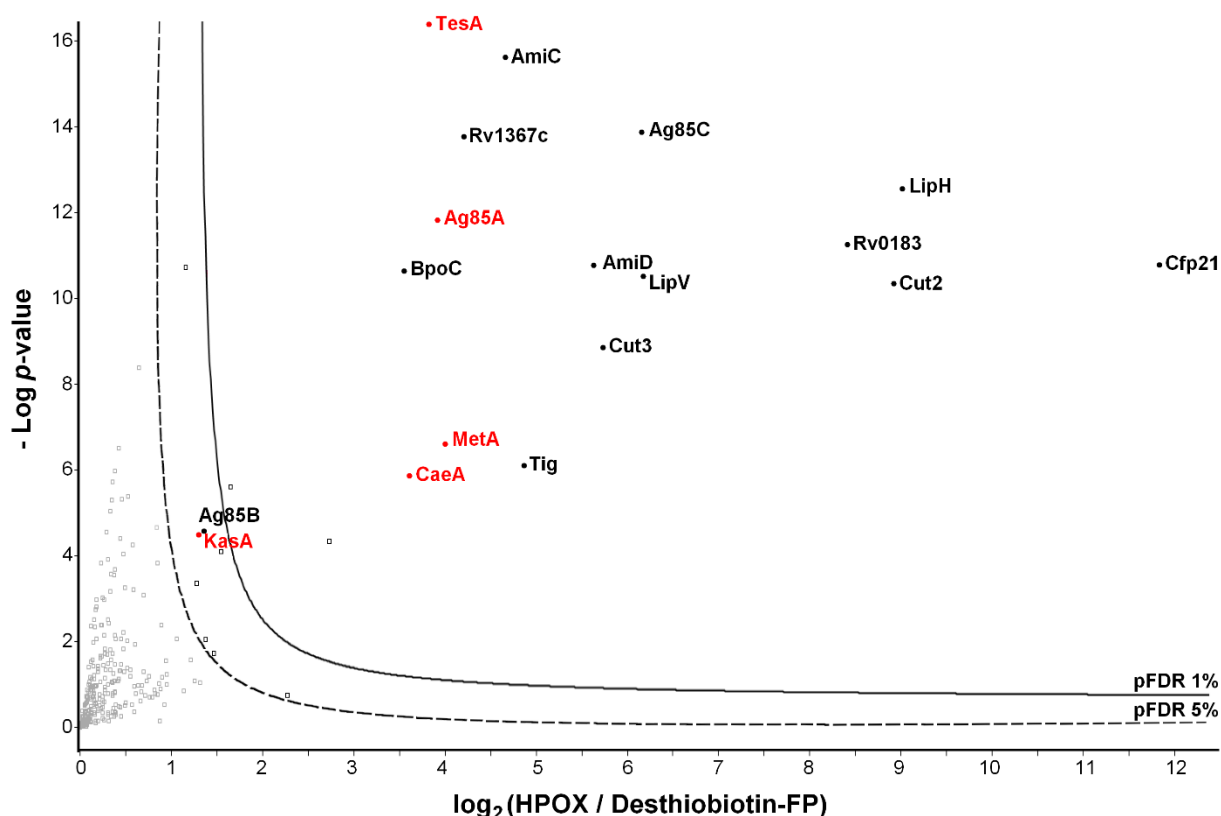


**Figure 4. Volcano plot of proteomic analysis of HPOX in *M. tb mc*<sup>26230</sup> culture.** Volcano plot showing the significance two-sample t-test (-Log p-value) versus fold-change (Log<sub>2</sub> (LFQ normalized intensity in HPOX versus Desthiobiotin-FP condition)) on the y and x axes, respectively. Here the plot is zoomed on the positive difference between the two conditions. The full line is indicative of protein hits obtained at a permutation false discovery rate of 1% (pFDR). Only protein hits obtained at a pFDR of 5% (dashed line) and with a score threshold value  $\geq 60$  were selected, and are highlighted in **black** (non-essential) or in **red** (essential). Data results from two different experiments processed three times.

As expected, the identified proteins targeted by **HPOX** were all (Ser/Cys)-based enzymes. Among them, a variety of Ser/Cys hydrolases were detected. These included the putative  $\beta$ -lactamase Rv1367c possibly involved in cell wall biosynthesis; two amidases AmiC (Rv2888c) and AmiD (Rv3375); BpoC (Rv0554) a putative serine hydrolase [43]; two members of the lipase family Lip (LipH [45] and LipV [46]); three Cutinase-like proteins (Cfp21, Cut2 and Cut3) [47]; and the monoacylglycerol lipase Rv0183 [48].

More interestingly, 5 out of 18 identified proteins have been annotated as essential enzymes [49] (**Table 3**). These include the antigen 85 complex, Ag85A (Rv3804c), Ag85B (Rv1886c) and Ag85C (Rv0129c) [50]; the thioesterase TesA (Rv2928) [51]; the carboxylesterase CaeA (Rv2224c) [52]; the beta-ketoacyl synthase KasA (Rv2245) [53]; and the sole putative  $\alpha/\beta$ -hydrolase MetA (Rv3341) belonging to the homoserine *O*-acetyltransferase family proteins in *M. tb* [54].

### 2.5 *TesA*, *Rv0183* and *Cfp21* are inhibited by **HPOX**.

In order to validate some targets of **HPOX** inhibitor, we further investigated its ability to efficiently inhibit the activity of three identified proteins; *i.e.*, *TesA*, *Cfp21* and *Rv0183*. Coding sequences were amplified from *M. tb* genome, cloned in *E. coli* and the enzymes produced in recombinant form and purified as previously reported [48, 55, 56]. Purified proteins were then individually incubated for 30 min at room temperature with **HPOX** at various inhibitor molar excess ( $x_I$ ). The residual enzyme activity was then measured using *para*-nitrophenyl caprylate (*pNPC-8*) as substrate for *TesA* [56] and *Cfp21* [55], and monoolein as substrate in the case of *Rv0183* [48]. The variation in the residual enzyme activity allowed determination of the inhibitor molar excess leading to 50% enzyme inhibition, *i.e.*,  $x_{I50}$  value [27, 57]. Thereby, a  $x_{I50}$  value of 0.5 is synonymous with a 1:1 stoichiometric ratio between the inhibitor and the lipolytic enzyme, and is therefore the highest level of inhibitory activity that can be achieved.

As depicted in **Figure 5**, a clear dose-dependent inhibition was observed with the three enzymes. TesA, Rv0183 and Cfp21 were indeed strongly inactivated, with 97.6% and 88.5% inhibition at  $x_1 = 20$ , respectively (**Figure 5**, inset). Interestingly, **HPOX** was found to react almost stoichiometrically with pure TesA and Rv0183 as confirmed by their respective  $x_{150}$  values of around 0.60. These results clearly demonstrate that these three lipolytic enzymes are effective targets of **HPOX**.

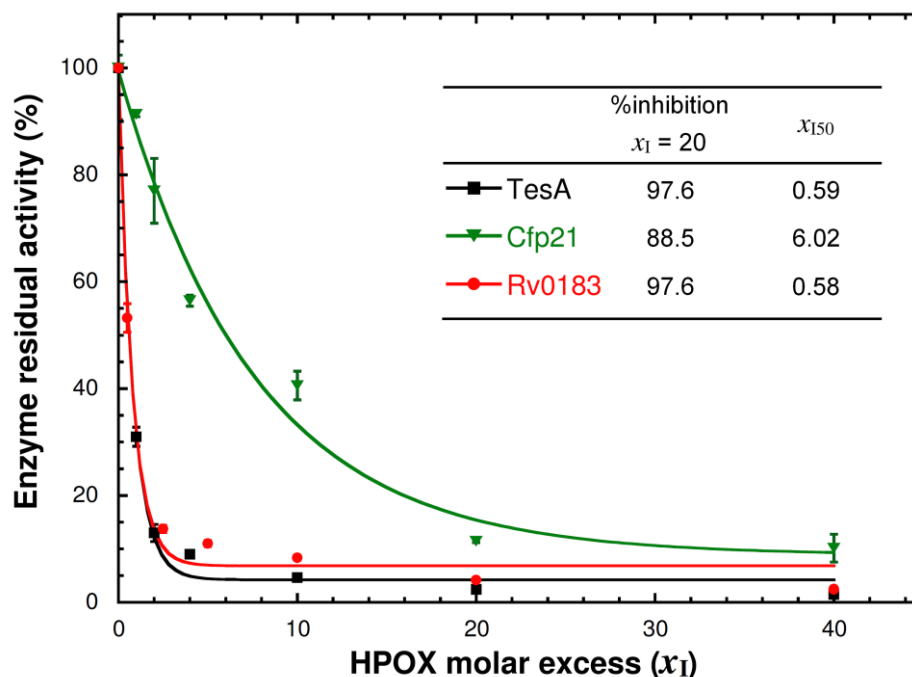


**Figure 5. HPOX efficiently impairs TesA, Cfp21 and Rv0183 activities *in vitro*.** Variation of the residual activities of TesA, Cfp21 and Rv0183 as a function of increasing molar excess ( $x_1$ ) of **HPOX**. Each enzyme was pre-incubated at various inhibitor molar excess ( $x_1$ ) for 30 min at 25 °C. The inset displays the determined values of  $x_{150}$  and the level of inhibition at  $x_1 = 20$ . Kinetic assays were performed as described in **Experimental Section**. Results are expressed as mean values  $\pm$  SD of at least two independent assays.

The fact that these **OXs** derivatives behave against *M. tb* extracellular growth similarly to two other well-known non-specific (Ser/Cys)-enzyme inhibitors, namely Orlistat (MIC  $\sim$  25  $\mu$ M) [41, 58] and the human lysosomal acid lipase inhibitor lalistat (MIC  $\sim$  25–50  $\mu$ M) [42], support the assumption that **HPOX**, and certainly all the other active **OX** compounds, may act as multi-target inhibitors by impairing the activities of multiple non-essential lipolytic enzymes as well as essential proteins involved in various important physiological pathways of *M. tb* life cycle.

Overall, it is now acknowledged that the lipolytic enzymes containing a catalytic Ser or Cys residue in their active site are not only involved in the host-pathogen cross-talk [59], but also play several roles in the physiopathology of the disease, in particular by recycling fatty acids from host lipids, a key element favoring *M. tb* reactivation [48, 60] and survival in dormancy [61]. *M. tb* indeed induces the formation of lipid bodies (LB) inside infected macrophages, giving the cells a foamy appearance. In foamy macrophages (FM), bacilli accumulate lipids within intracytoplasmic lipid inclusions (ILI) [62-65], which allow the bacteria to persist in a non-replicating state. In FM, several mycobacterial lipolytic enzymes of *M. tb* hydrolyze host triacylglycerols (TAG) from LB and the resulting fatty acids are stored within ILI as newly synthesized TAGs. Consequently, although they exhibited moderate MIC<sub>50</sub> values against *M. tb* H37Rv as compared to classical antibiotics or the more recent CyC analogs [31]; **OX** compounds may however represent attractive chemical tools for identifying such (Ser/Cys)-containing enzymes in living mycobacteria, studying the regulation of ILI formation in infected FM [66], and thus provide a better understanding of how bacilli can persist inside lipid-rich FM.

### 3. Conclusion

In conclusion, we have developed a new series of promising oxadiazolone-core compounds, active against three pathogenic mycobacteria. By blocking extracellular and/or intracellular *M. tb* growth, we anticipate that these **OX** probes could thus provide interesting insights in the mechanisms operating during mycobacterial replication, persistence and/or reactivation, which are major issues for deciphering the susceptibility and the general development of TB. Moreover, as these compounds target bacterial pathway yet unexploited by anti-TB compounds, the identification of the mycobacterial enzymes inhibited by these **OX** compounds *in vivo* may contribute to background information for the development of new therapeutic strategies for elimination of either actively replicating or latent bacilli from infected individuals. Accordingly, given the importance of such

(Ser/Cys)-enzymes for *M. tb* viability during infection, they should represent new attractive drug targets. Such experiments are currently underway, and will be reported in due course.

## 4. Experimental Section

### 4.1. Chemistry.

The first 13 oxadiazolone derivatives **5a-k**, **6k** and **7k** were synthesized as described previously [27, 67]. The new six derivatives **6a,d,e** and **7a,d,e** were prepared from commercial (4-phenoxyphenyl)hydrazine hydrochloride (**2**) and phenylhydrazine hydrochloride (**3**), respectively, by performing both the coupling reaction with alkyl chloroformate **2a-k** (step i) and the cyclization reaction with diphosgene (step ii) in a one-pot two-steps reaction [27]. All compound were at least 98% pure as determined by HPLC analysis [27]. Stock solutions (4 mg/mL) in which the oxadiazolone compounds were found to be completely soluble in dimethyl sulfoxide (DMSO), were prepared prior to drug susceptibility testing. See *Supplementary Material* for NMR, HPLC analysis and HRMS spectra of the new six **OX** derivatives.

#### 4.1.1 General procedure for the one step preparation of 5-alkoxy-3-aryl-1,3,4-oxadiazol-2(3H)-one compounds.

4.1.1.1. 5-(2-(benzyloxy)ethoxy)-3-(3-phenoxyphenyl)-1,3,4-oxadiazol-2(3H)-one (**6a** = **BepPPOX**). (4-phenoxyphenyl)hydrazine hydrochloride [67] **2** (8.2 g, 34.6 mmol, 1 equiv.) and 1-methyl pyrrolidone (2.41 ml, 31.1 mmol, 0.9 equiv.) were dissolved in dry pyridine (700 mL). The solution was cooled in an ice bath to 0 °C. Then, 2-benzyloxyethyl chloroformate **4a** (6.87 mL, 38.6 mmol, 1.1 equiv.) was added dropwise over a period of 30 min at 0-5 °C and allowed to stir for 1 h at 0 °C and 1 h at room temperature. The reaction mixture was diluted by addition of methylene chloride (300 mL) and dry pyridine (70 mL) and the mixture was cooled at -10 °C using an ice-salt bath. A solution of diphosgene (6.26 mL, 51.8 mmol, 1.5 equiv.) in methylene chloride (30 mL) was added dropwise using a syringe pump over a period of 1 h while maintaining -10 °C with an ice-salt bath.

After the addition is complete the reaction mixture stirred 1 h at -10 °C and 2 h at room temperature. The reaction mixture was diluted with water (1 L) and extracted with diethyl ether (3× 250 mL). The combined organic layers were washed with water (2× 250 mL) and brine (3× 100 mL), dried over MgSO<sub>4</sub>, and filtered. Purification by column chromatography using cyclohexane/ethyl acetate (98/2 to 95/5, v/v) as eluent gave the title compound **6a** (**BepPPOX**) as a yellow oil (9.94 g, 71%). Analytical data for **BepPPOX**:  $R_f$  (AcOEt/Cyclohexane 1:3, v/v) 0.36. HRMS (ESI)  $m/z$  [M+H]<sup>+</sup> calcd. for C<sub>23</sub>H<sub>21</sub>N<sub>2</sub>O<sub>5</sub>: 405.1445 Da ; found : 405.1446 Da. <sup>1</sup>H NMR δ 7.71 (dd,  $J = 9.1$  Hz,  $J = 2.2$  Hz, 2H), 7.31 (m, 7H), 6.98-7.13 (m, 5H), 4.60 (s, 2H), 4.54 (m, 2H), 3.83 (m, 2H). <sup>13</sup>C NMR δ 157.14 (s), 155.23 (s), 154.77 (s), 148.29 (s), 137.43 (s), 131.56 (s), 129.85 (2 × d), 128.55 (2 × d), 127.99 (d), 127.79 (2 × d), 123.47 (d), 119.83 (2 × d), 119.47 (2 × d), 118.74 (2 × d), 73.42 (t), 70.56 (t), 66.99 (t).

4.1.1.2. *5-isoButyloxy-3-(4-phenoxyphenyl)-1,3,4-oxadiazol-2(3H)-one* (**6d** = **iBpPPOX**). Prepared using Isobutyl chloroformate **4d** applying similar method as described above for **6a**. Analytical data for **iBpPPOX**: pale yellow oil (87%).  $R_f$  (AcOEt/Cyclohexane 1:3, v/v) 0.55. HRMS (ESI)  $m/z$  [M+H]<sup>+</sup> calcd. for C<sub>18</sub>H<sub>19</sub>N<sub>2</sub>O<sub>4</sub>: 327.1339 Da ; found : 327.1342 Da. <sup>1</sup>H NMR δ 7.72 (dd,  $J = 9.2$  Hz,  $J = 2.3$  Hz, 2H), 7.30 (m, 2H), 6.97-7.12 (m, 5H), 4.14 (t,  $J = 6.6$  Hz, 2H), 2.15 (m, 1H), 1.0 (d, 6H). <sup>13</sup>C NMR δ 157.17 (s), 155.42 (s), 154.67 (s), 148.36 (s), 131.66 (s), 129.83 (2 × d), 123.42 (d), 119.79 (2 × d), 119.49 (2 × d), 118.69 (2 × d), 71.39 (t), 22.75 (t), 18.70 (2 × q).

4.1.1.3. *5-Hexyloxy-3-(4-phenoxyphenyl)-1,3,4-oxadiazol-2(3H)-one* (**6e** = **HpPPOX**). Prepared using Hexyl chloroformate **4e** applying similar method as described above for **6a**. Analytical data for **HpPPOX**: yellow oil (85%).  $R_f$  (AcOEt/Cyclohexane 1:3, v/v) 0.95. HRMS (ESI)  $m/z$  [M+H]<sup>+</sup> calcd. for C<sub>20</sub>H<sub>23</sub>N<sub>2</sub>O<sub>4</sub>: 355.1652 Da ; found : 355.1652 Da. <sup>1</sup>H NMR δ 7.72 (dd,  $J = 9.0$  Hz,  $J = 2.0$  Hz, 2H), 7.30 (m, 2H), 6.97-7.12 (m, 5H), 4.37 (t,  $J = 6.6$  Hz, 2H), 1.80 (m, 2H), 1.30-1.58 (m, 6H), 0.90 (t,  $J = 6.8$  Hz, 3H). <sup>13</sup>C NMR δ 157.16 (s), 155.33 (s), 154.67 (s), 148.38 (s), 131.65 (s),

129.83 (2 × d), 123.42 (d), 119.78 (2 × d), 119.49 (2 × d), 118.68 (2 × d), 71.79 (t), 31.36 (t), 28.35 (t), 25.17 (t), 22.50 (t), 13.99 (q).

4.1.1.4. *5-Benzyloxyethoxy-3-phenyl-1,3,4-oxadiazol-2(3H)-one (7a = BePOX)*. Prepared using 2-benzyloxyethyl chloroformate **4a** and phenylhydrazine hydrochloride **3** applying similar method as described above for **6a**. Analytical data for **BePOX**: pale yellow oil (79%).  $R_f$  (AcOEt/Cyclohexane 1:3,  $v/v$ ) 0.36. HRMS (ESI)  $m/z$   $[M+H]^+$  calcd. for  $C_{17}H_{17}N_2O_4$ : 313.1183 Da ; found : 313.1183 Da.  $^1H$  NMR  $\delta$  7.75 (m, 2H), 7.18-7.73 (m, 8H), 4.60 (s, 2H), 4.54 (m, 2H), 3.83 (m, 2H).  $^{13}C$  NMR  $\delta$  155.23 (s), 148.23 (s), 137.44 (s), 136.17 (s), 129.12 (2 × d), 128.55 (2 × d), 127.98 (d), 127.79 (2 × d), 125.56 (d), 117.95 (2 × d), 73.41 (t), 70.55 (t), 66.98 (t).

4.1.1.5. *5-isoButyloxy-3-phenyl-1,3,4-oxadiazol-2(3H)-one (7d = iBPOX)*. Prepared using Isobutyl chloroformate **4d** and phenylhydrazine hydrochloride **3** applying similar method as described above for **6a**. Analytical data for **iBPOX**: white crystals (77%). Mp: 76-77°C.  $R_f$  (AcOEt/Cyclohexane 1:3,  $v/v$ ) 0.55. HRMS (ESI)  $m/z$   $[M+Na]^+$  calcd. for  $C_{12}H_{14}N_2O_3Na$ : 257.0897 Da ; found : 257.0895 Da.  $^1H$  NMR  $\delta$  7.80 (m, 2H), 7.42 (m, 2H), 7.25 (m, 1H), 4.18 (d,  $J = 6.6$  Hz, 2H), 1.85 (m, 1H), 1.05 (d, 6H).  $^{13}C$  NMR  $\delta$  155.63 (s), 148.51 (s), 136.44 (s), 129.29 (2 × d), 125.67 (d), 118.14 (2 × d), 77.57 (t), 27.94 (d), 18.89 (2 × q).

4.1.1.6. *5-Hexyloxy-3-phenyl-1,3,4-oxadiazol-2(3H)-one (7e = HPOX)*. Prepared using Hexyl chloroformate **4e** and phenylhydrazine hydrochloride **3** applying similar method as described above for **6a**. Analytical data for **HPOX**: white crystals (71%). Mp: 34-35°C.  $R_f$  (AcOEt/Cyclohexane 1:3,  $v/v$ ) 0.59. HRMS (ESI)  $m/z$   $[M+H]^+$  calcd. for  $C_{14}H_{19}N_2O_3$ : 263.1390 Da ; found : 263.1390 Da.  $^1H$  NMR  $\delta$  7.80 (ddd,  $J = 8.4$  Hz,  $J = 2.3$  Hz,  $J = 0.75$  Hz, 2H), 7.42 (dd,  $J = 7.6$  Hz,  $J = 1.7$  Hz, 2H), 7.22 (t,  $J = 7.4$  Hz, 1H), 4.40 (t,  $J = 6.6$  Hz, 2H), 1.85 (m, 2H), 1.33-1.49 (m, 6H), 0.93 (t, 3H).  $^{13}C$  NMR  $\delta$  155.54 (s), 148.53 (s), 136.45 (s), 129.30 (2 × d), 125.67 (d), 118.13 (2 × d), 71.97 (t), 31.45 (t), 28.55 (t), 25.36 (t), 22.68 (t), 14.17 (q).

## 4.2. Biological evaluation

### 4.2.1. Bacterial strains and growth condition.

*M. marinum* ATCC BAA-535/M, *M. bovis* BCG Pasteur 1173P2 and *M. tb* mc<sup>2</sup>6230 (H37Rv  $\Delta$ RD1  $\Delta$ panCD [28]) strains were routinely grown in Middlebrook 7H9 broth (BD Difco) supplemented with 0.2% glycerol, 0.05% Tween 80 (Sigma-Aldrich), 10% oleic acid, albumin, dextrose, catalase (OADC enrichment; BD Difco) (7H9-S) and 24  $\mu$ g/mL D-pantothenate (*M. tb* mc<sup>2</sup>6230). For further intra and extracellular assays, *M. tb* H37Rv expressing GFP [36] was grown for 14 days in 7H9-S supplemented with 50  $\mu$ g/mL hygromycin B (Euromedex). All cultures were kept at 37 °C without shaking, except *M. marinum* which was grown at 32 °C.

### 4.2.2. Susceptibility testing on *M. marinum*, *M. bovis* BCG and *M. tb* mc<sup>2</sup>6230.

The concentrations of compound leading to 50% of bacterial growth (MIC<sub>50</sub>) were first determined using the resazurin microtiter assay (REMA) [29, 30]. Briefly, log-phase bacteria were diluted to a cell density of  $5 \times 10^6$  cells/mL and 100  $\mu$ L of this inoculum was grown in a 96-well plate in the presence of serial dilutions of compounds. After 7-14 days incubation, 20  $\mu$ L of a 0.025% (w/v) resazurin solution was added to each well (200  $\mu$ L) and incubation was continued until the appearance of a color change (from blue to pink) in the control well (bacteria without antibiotics). Fluorescence of the resazurin metabolite resorufin ( $\lambda_{\text{excitation}}$ , 530 nm;  $\lambda_{\text{emission}}$ , 590 nm) was then measured [30] and the concentration leading to 50% growth inhibition was defined as the MIC<sub>50</sub>. See *Supplementary Material* for detailed protocol.

### 4.2.3. High-content screening assay - Extracellular assay.

A 14 days old culture of *M. tb* H37Rv-GFP was washed twice with PBS and resuspended in 7H9 medium containing 10% OADC, 0.5% glycerol, 0.05% Tween 80 and 50  $\mu$ g/mL hygromycin B. Bacteria were seeded in 384 well plates ( $7 \times 10^5$  bacteria/mL) containing 2-fold dilutions of the compounds in DMSO. The final volume of DMSO was kept under 0.3%. Plates were incubated at

37 °C, 5% CO<sub>2</sub> for 5 days. Bacterial fluorescence levels (RFU) were recorded using a fluorescent microplate reader (Victor X3, Perkin-Elmer). The MIC<sub>50</sub> of all tested compounds were determined using ten-point dose-response curves. In each plate, negative control with 1% DMSO; and positive controls containing 1 µg/mL INH and RIF were also included.

#### 4.2.4. High-content screening assay in infected macrophages - Intracellular assay.

The growth of *M. tb* H37Rv-GFP strain in macrophages was monitored by automated fluorescence confocal microscope (Opera, Perkin-Elmer) as already described [36, 68]. Briefly, bacteria were washed twice with PBS and resuspended in RPMI 1640 medium (Invitrogen) supplemented with 10% heat-inactivated fetal bovine serum (FBS, Invitrogen). Murine (Raw264.7) macrophages (American Type Culture Collection TIB-71) were infected at a multiplicity of infection (MOI) of 2:1 and incubated 2 hours at 37 °C in RPMI 1640 medium containing 10% FBS. Cells were then washed, treated with 50 µg/mL amikacin (Euromedex) for 1 hour at 37 °C to kill all extra-cellular bacteria, washed again and finally seeded in 384-well plates ( $5 \times 10^5$  cells/mL), containing 2-fold dilutions of compounds in DMSO. The final volume of DMSO was kept under 0.3%. Plates were incubated for 5 days at 37 °C, 5% CO<sub>2</sub>. Infected cells were stained for 30 min using Syto60 dye (Invitrogen) at a final concentration of 5 µM before reading using fluorescence confocal microscope (20X water objective; GFP:  $\lambda_{\text{ex}}$  488 nm,  $\lambda_{\text{em}}$  520 nm; Syto60:  $\lambda_{\text{ex}}$  640 nm,  $\lambda_{\text{em}}$  690 nm). Dose-responses were fitted using Prism software (sigmoidal dose-response, variable slope model). The MIC<sub>50</sub> was determined using ten-point dose-response curves as an average of the MIC<sub>50</sub> of 4 parameters, the ratio of infected cells, the total area of bacteria, the cells number and the bacterial area per infected cell. In each plate, negative control with 1% DMSO (*i.e.*, infected macrophages only); as well as positive controls containing 10 µg/mL INH, ETO and RIF were also included.

### 4.3. HPOX target enzymes identification

4.3.1. Activity-based protein profiling (ABPP). Homogeneous bacterial suspension of *M. tb* mc<sup>2</sup>6230 in 7H9-S was adjusted at an OD<sub>600</sub> of 60 and then incubated with the selected **HPOX**

inhibitor (400  $\mu$ M final concentration) or DMSO (control) at 37 °C for 2-3 h. under gentle shaking at 75 rpm. Bacteria were then washed 3 times with PBS containing 0.05% Tween 80, resuspended in PBS buffer at a 1:1 (*w/v*) ratio and then lysed by mechanical disruption on a BioSpec Beadbeater. Both **HPOX**-treated *M. tb* mc<sup>2</sup>6230 and DMSO-control lysate samples (750  $\mu$ L – 0.75 mg total proteins) were labeled with 2  $\mu$ M Desthiobiotin-FP probe for 90 min at room temperature. Samples were enriched for biotinylated proteins using Nanolink streptavidin magnetic beads 0.8  $\mu$ m (Solulink), according to the manufacturer's instructions. The resulting captured biotinylated proteins solution was mixed with 5X Laemmli reducing sample buffer, and heated at 95 °C for 5 min. The released denatured proteins were subjected to tryptic digestion, peptide extraction, and LC-MS/MS analysis as described below.

Alternatively, the **HPOX**-treated *M. tb* mc<sup>2</sup>6230 and DMSO-control lysate samples (100  $\mu$ L – 100  $\mu$ g total proteins) were incubated with 2  $\mu$ M ActivX TAMRA-FP probe (Thermo Fisher Scientific) for 90 min at room temperature and in absence of light. The reaction was stopped by adding 5X Laemmli reducing sample buffer and boiling at 95 °C for 5 min. The labeled proteins were further separated by SDS-PAGE electrophoresis. TAMRA fluorescence (TAMRA:  $\lambda_{\text{ex}}$  557 nm,  $\lambda_{\text{em}}$  583 nm) was detected using a ChemiDoc MP Imager (Bio-Rad). Detailed Materials and Methods is given in *Supplementary Material*.

*4.3.2. Protein identification and quantification.* Protein extract were loaded and stacked on a NuPAGE gel (Life Technologies). Stained bands were submitted to an in-gel trypsin digestion [69]. Peptides extracts were reconstituted with 0.1% trifluoroacetic acid in 4% acetonitrile and analyzed by liquid chromatography (LC)-tandem mass spectrometry (MS/MS) using an Orbitrap Fusion Lumos Tribrid Mass Spectrometer (Thermo Electron, Bremen, Germany) online with a an Ultimate 3000RSLC nano chromatography system (Thermo Fisher Scientific, Sunnyvale, CA). Protein identification and quantification were processed using the MaxQuant computational proteomics platform, version 1.5.3.8 [70] using a UniProt *M. tuberculosis* ATCC 25618 database (date 2018.01; 2164 entries). The statistical analysis was done with Perseus program (version 1.5.6.0).

Differential proteins were detected using a two-sample *t*-test at 0.01 and 0.05 permutation based FDR. The mass spectrometry proteomics data, including search results, have been deposited to the ProteomeXchange Consortium ([www.proteomexchange.org](http://www.proteomexchange.org)) [71] via the PRIDE partner repository with the dataset identifier PXD010255 (Reviewer account details. **username:** reviewer87937@ebi.ac.uk / **password:** Hhpb9H0Y). Detailed Materials and Methods is given in *Supplementary Material*.

#### 4.4. Inhibition assays on pure recombinant proteins.

The three lipolytic enzymes from *M. tb*, the thioesterase TesA, the monoacylglycerol lipase Rv0183, and the Cutinase-like protein Cfp21 were produced and purified as previously reported [48, 55, 56].

The lipase–inhibitor pre-incubation method was used to test, in aqueous medium and in the absence of substrate, the possible direct reactions between lipases and inhibitors as previously described [27, 57, 72]. Briefly, an aliquot of each enzyme was pre-incubated at 25 °C with **HPOX** at various inhibitor molar excess ( $x_1$ ) ranging from 1 to 40 related to 1 mol of enzyme. A sample of the incubation medium was collected after 30 min incubation period and the residual enzyme activity was measured. The variation in the residual lipase activity allowed determination of the inhibitor molar excess which reduced the enzyme activity to 50% of its initial value ( $x_{150}$ ) [27, 57, 72]. In each case, control experiments were performed in the absence of inhibitor. The respective enzymatic activity of TesA and Cfp21 were assessed using *para*-nitrophenyl (*p*NP) ester assay with *p*NP caprylate (*p*NP-C8) as substrate, as described previously [23]. Rv0183 residual activity was determined using monoolein as substrate, as reported in [48, 57]. Dose-response curves were fitted in Kaleidagraph 4.2 Software (Synergy Software). Results are expressed as mean values  $\pm$  SD of at least two independent assays.

## Figure captions

**Figure 1.** Chemical structure of (A) 5-(pyridin-4-yl)-1,3,4-oxadiazol-2(3*H*)-one **S57**, and (B) 5-methoxy-3-(3-phenoxyphenyl)-1,3,4-oxadiazol-2(3*H*)-one **MmPPOX** and its mode of action. (C) General procedure for the one step preparation of 5-alkoxy-3-phenyl substituted-1,3,4-oxadiazol-2(3*H*)-one compounds from either (3-phenoxyphenyl)hydrazine hydrochloride (**1**), (4-phenoxyphenyl)hydrazine hydrochloride (**2**) or phenylhydrazine hydrochloride (**3**), giving **OX** derivatives **5a-k** (*i.e.*, **RmPPOX**), **6a,d,e,k** (*i.e.*, **RpPPOX**) or **7a,d,e,k** (*i.e.*, **RPOX**), respectively. Reagents and conditions: i) Alkyl chloroformate **4a-k**, Pyridine, 0 °C to RT; ii) ClCO<sub>2</sub>CCl<sub>3</sub>, CHCl<sub>2</sub>, Pyridine, 0 °C to RT, 40-85%. Adapted from [27].

**Figure 2.** *In vitro* and *ex vivo* dose-response activity of the **OX** derivatives against *M. tb* **H37Rv**. (A) Activity of **BePOX**, **iBpPPOX** and **HPOX** against GFP-expressing *M. tb* replicating in broth medium, expressed as normalized relative fluorescence units (RFU%). The dashed line represents the level of inhibition (~70%) reached with 1 µg/mL (=7.3 µM) INH as control. The MIC<sub>50</sub> of **BePOX**, **iBpPPOX** and **HPOX** replicating in culture broth medium were 30.8 µM, 32.0 µM and 44.6 µM, respectively. (B) Activity of **iBpPPOX**, **BePPOX**, **HpPPOX** and **iBPOX** against *M. tb* replicating inside Raw264.7 macrophages. Results are expressed as the percentage of infected macrophages after 5 days post-infection. The dashed line represents the level of inhibition (~87%) reached with 10 µg/mL (=73 µM) INH as control. The MIC<sub>50</sub> of **BePPOX**, **iBpPPOX**, **HpPPOX** and **iBPOX** replicating inside macrophages were 3.5 µM, 8.5 µM, 9.5 µM and 17.1 µM, respectively. Each value is the mean ± SD for a triplicated dose-response. Experiments were conducted at least twice with consistent results.

**Figure 3.** Activity based protein profiling (ABPP) workflow for the identification of the proteins covalently bound to **OX** inhibitors. (A) Cell culture of *M. tb* mc<sup>2</sup>6230 was pre-treated with selected **HPOX** inhibitor prior to cell lysis and further incubation with TAMRA-FP or

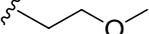
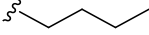
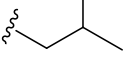
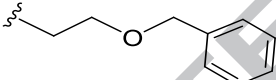
Desthiobiotin-FP probe. In this latter case, samples were then treated with streptavidin-magnetic beads for the capture and enrichment of labelled proteins. **(B-C)** Equal amounts of proteins obtained in **A** were separated by SDS-PAGE and visualized by in-gel fluorescence (*right* panel - lanes D-E: TAMRA detection) or silver staining (*left* panel – lanes A-C). Enzymes whose TAMRA-FP labelling is impeded because of the presence of **HPOX** in their active-site are shown by arrowheads. **(D)** Tryptic digestion followed by tandem mass spectrometry analyses and subsequent differential proteomics analysis allowed identifying the target proteins.

**Figure 4. Volcano plot of proteomic analysis of HPOX in *M. tb* mc<sup>2</sup>6230 culture.** Volcano plot showing the significance two-sample t-test (-Log p-value) *versus* fold-change (Log<sub>2</sub> (LFQ normalized intensity in HPOX *versus* Desthiobiotin-FP condition)) on the y and x axes, respectively. Here the plot is zoomed on the positive difference between the two conditions. The full line is indicative of protein hits obtained at a permutation false discovery rate of 1% (pFDR). Only protein hits obtained at a pFDR of 5% (dashed line) and with a score threshold value  $\geq 60$  were selected, and are highlighted in **black** (non-essential) or in **red** (essential). Data results from two different experiments processed three times.

**Figure 5. HPOX efficiently impairs TesA, Cfp21 and Rv0183 activities *in vitro*.** Variation of the residual activities of TesA, Cfp21 and Rv0183 as a function of increasing molar excess ( $x_1$ ) of **HPOX**. Each enzyme was pre-incubated at various inhibitor molar excess ( $x_1$ ) for 30 min at 25 °C. The inset displays the determined values of  $x_{150}$  and the level of inhibition at  $x_1 = 20$ . Kinetic assays were performed as described in **Experimental Section**. Results are expressed as mean values  $\pm$  SD of at least two independent assays.

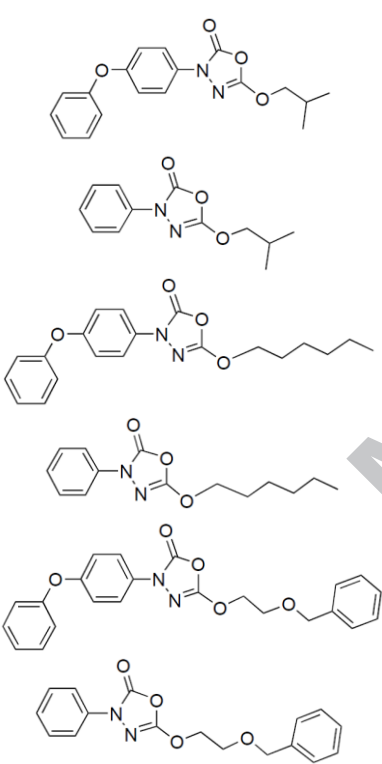
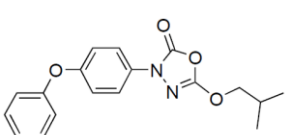
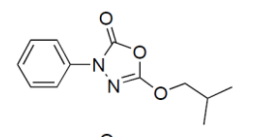
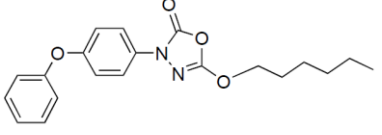
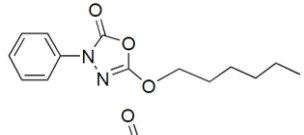
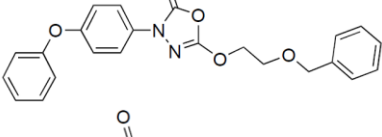
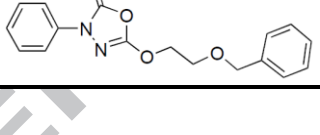
## Tables

**Table 1.** Antibacterial activities of the oxadiazolone derivatives against *M. marinum*, *M. Bovis* BCG and *M. tb mc<sup>2</sup>6230* using the REMA method <sup>a</sup>

Compounds		MIC <sub>50</sub> (μM)		
		<i>M. marinum</i>	<i>M. bovis</i> BCG	<i>M. tb mc<sup>2</sup>6230</i>
INH		20.5	0.71	1.5
RIF		1.4	0.027	0.015
<b>MmPPOX</b>		7.0	15.0	71.3
<b>MpPPOX</b>		11.5	39.9	>120
<b>MPOX</b>		52.9	>120	89.8
<b>EmPPOX</b>		3.4	7.1	>120
<b>MemPPOX</b>		2.7	9.4	91.2
<b>BmPPOX</b>		4.1	6.6	52.2
<b>iBmPPOX</b>		13.6	4.4	57.2
<b>iBpPPOX</b>		6.9	8.5	<b>31.1</b>
<b>iBPOX</b>		2.5	5.7	>120
<b>HmPPOX</b>		11.1	5.8	48.8
<b>HpPPOX</b>		3.4	14.0	41.3
<b>HPOX</b>		2.6	<b>3.5</b>	40.5
<b>BemPPOX</b>		5.6	10.5	49.5
<b>BepPPOX</b>		10.1	18.5	44.5
<b>BePOX</b>		<b>1.9</b>	6.6	33.2
<b>OmPPOX</b>		8.0	11.0	44.7
<b>EhmPPOX</b>		8.3	8.1	43.3
<b>DmPPOX</b>		10.5	80.8	>120
<b>DomPPOX</b>		19.5	22.6	>120

<sup>a</sup> Experiments were performed as described in **Experimental Section**. MIC<sub>50</sub>: compound minimal concentration leading to 50% of growth inhibition, as determined by the REMA assay. The best MIC<sub>50</sub> obtained for each strain are highlighted in bold. Values are mean of at least two independent assays performed in triplicate. INH, isoniazid; RIF, rifampicin.

**Table 2.** Antitubercular activities of the most active **OX** derivatives against *M. tb* H37Rv <sup>a</sup>

Compounds		Extracellular growth	Intracellular macrophage growth <sup>b</sup>	
		MIC <sub>50</sub> (μM)	MIC <sub>50</sub> (μM)	CC <sub>50</sub> (μM)
INH <sup>c</sup>		1.2	1.2	>150
RIF <sup>c</sup>		0.01	2.9	24
ETO <sup>c</sup>		6.0	6.0	120
<b>iBpPOX</b>		32.0	8.5	>100
<b>iBPOX</b>		>50	17.1	>100
<b>HpPOX</b>		>50	9.5	>100
<b>HPOX</b>		44.6	No effect	>100
<b>Be<sub>p</sub>POX</b>		>50	3.5	>100
<b>BePOX</b>		30.8	No effect	>100

<sup>a</sup> Experiments were performed as described in **Experimental Section**. MIC<sub>50</sub>: compound minimal concentration leading to 50% of growth inhibition. CC<sub>50</sub>: compound concentration leading to 50% of cell cytotoxicity. Each value is the mean ± SD for a triplicated dose-response. Experiments were conducted at least twice with consistent results. <sup>b</sup> Raw264.7 macrophages were infected by *M. tb* H37Rv-GFP at a MOI of 2:1. <sup>c</sup> Data from [36]. INH, isoniazid; RIF, rifampicin; ETO, ethionamide.

**Table 3.** HPOX target proteins identified in *M. tb* mc<sup>2</sup>6230 culture by LC-ESI-MS/MS analysis. <sup>a</sup>

Protein name	Rv number	Mol. weight [kDa]	Essentiality	Location <sup>b</sup>	Function	Functional Category <sup>c</sup>
Cutinase <b>Cfp21</b>	Rv1984c	21.8		CF; CW; M	Lipase/esterase	CW/CP
Probable cutinase <b>Cut2</b>	Rv2301	23.9		M, WCL, CF	hydrolase	CW/CP
Probable cutinase <b>Cut3</b>	Rv3451	26.5		M, CF	hydrolase	CW/CP
Lipase <b>LipV</b>	Rv3203	27.9		WCL	Lipase/esterase	IM/R
Non-heme bromoperoxidase <b>BpoC</b>	Rv0554	28.4		M	hydrolase	V/D/A
Thioesterase <b>TesA</b>	Rv2928	29.2	<i>in vitro</i> growth	M	Lipase/esterase	LM
Monoglyceride lipase <b>Rv0183</b>	Rv0183	30.3		M	Lipase/esterase	IM/R
Lipase <b>LipH</b>	Rv1399c	33.9		M	Lipase/esterase	IM/R
Secreted antigen 85-B FbpB ( <b>Ag85B</b> )	Rv1886c	34.6		CF; CW; M	Lipase/esterase	LM
Secreted antigen 85-A FbpA ( <b>Ag85A</b> )	Rv3804c	35.7	<i>in vitro</i>	CF; CW; M	Lipase/esterase	LM
Secreted antigen 85-C FbpC ( <b>Ag85C</b> )	Rv0129c	36.8		CF; CW	Lipase/esterase	LM
Probable homoserine O-acetyltransferase <b>MetA</b>	Rv3341	39.8	essential gene	M	Acyltransferase	IM/R
$\beta$ -ketoacyl-ACP synthase <b>KasA</b>	Rv2245	43.3	essential gene	CF; CW; M	Lipase/esterase	LM
Hypothetical protein <b>LH57_07490</b>	Rv1367c	43.7		M	$\beta$ -lactamase	CW/CP
Trigger factor <b>Tig</b>	Rv2462c	50.6		M, WCL, CF	Protein export	CW/CP
Amidase <b>AmiD</b>	Rv3375	50.6		CW; M	Amidase	IM/R
Amidase <b>AmiC</b>	Rv2888c	50.9		CW; M	Amidase	IM/R
Putative Carboxylesterase A <b>CaeA</b>	Rv2224c	55.9	Macrophage and <i>in vitro</i>	M, WCL, CF	Lipase/esterase	CW/CP

<sup>a</sup> Only positive hits with a pFDR of 5% and a score threshold value  $\geq 60$  were selected. <sup>b</sup> CF: Culture filtrate; CW: Cell wall; M: Membrane fraction; WCL: Whole cell lysate. <sup>c</sup> IM/R: Intermediary metabolism/respiration; CW/CP: cell wall/cell processes; LM: Lipid metabolism; V/D/A: Virulence, detoxification, adaptation.

## Acknowledgements

This work was supported by the CNRS and Aix-Marseille University. PCN was supported by a PhD Training program from the University of Science and Technology of Hanoi (837267E). Financial support to PB, VD and VL was provided by the European Community (ERC-STG INTRACELLTB n° 260901, MM4TB n°260872, CycloNHit n° 608407), the Agence Nationale de la Recherche (ANR-10-EQPX-04-01, ANR-14-CE08-0017), the Feder (12001407 (D-AL) Equipex Imaginex BioMed), the Région Nord Pas de Calais (convention n° 12000080). Proteomics analysis was supported by the Institut Paoli-Calmettes and the Centre de Recherche en Cancérologie de Marseille. Proteomic analyses were done using the mass spectrometry facility of Marseille Proteomics ([marseille-proteomique.univ-amu.fr](http://marseille-proteomique.univ-amu.fr)) supported by IBISA (Infrastructures Biologie Santé et Agronomie), Plateforme Technologique Aix-Marseille, the Cancéropôle PACA, the Provence-Alpes-Côte d'Azur Région, the Institut Paoli-Calmettes and the Centre de Recherche en Cancérologie de Marseille. VD is currently supported by the French Ministry of Foreign Affairs, the Korean Ministry of Science (MSIT) through the National Research Foundation of Korea (NRF, grant numbers 2017M3A9G6068246 and 2015R1C1A1A01053355) as well as the Gyeonggi province, Korea.

## Supplementary Material

Supplementary data associated with this article can be found, in the online version.

## References

- [1] WHO, Global tuberculosis report, [http://www.who.int/tb/publications/global\\_report/en/](http://www.who.int/tb/publications/global_report/en/) (2017).
- [2] A.I. Zumla, S.H. Gillespie, M. Hoelscher, P.P. Philips, S.T. Cole, I. Abubakar, T.D. McHugh, M. Schito, M. Maeurer, A.J. Nunn, New antituberculosis drugs, regimens, and adjunct therapies: needs, advances, and future prospects, *The Lancet. Infectious diseases*, 14 (2014) 327-340.
- [3] M. Pai, M.A. Behr, D. Dowdy, K. Dheda, M. Divangahi, C.C. Boehme, A. Ginsberg, S. Swaminathan, M. Spigelman, H. Getahun, D. Menzies, M. Raviglione, Tuberculosis, *Nature Reviews Disease Primers*, 2 (2016) 16076.
- [4] K. Andries, P. Verhasselt, J. Guillemont, H.W. Gohlmann, J.M. Neefs, H. Winkler, J. Van Gestel, P. Timmerman, M. Zhu, E. Lee, P. Williams, D. de Chaffoy, E. Huitric, S. Hoffner, E. Cambau, C. Truffot-Pernot, N. Lounis, V. Jarlier, A diarylquinoline drug active on the ATP synthase of *Mycobacterium tuberculosis*, *Science*, 307 (2005) 223-227.
- [5] M. Matsumoto, H. Hashizume, T. Tomishige, M. Kawasaki, H. Tsubouchi, H. Sasaki, Y. Shimokawa, M. Komatsu, OPC-67683, a nitro-dihydro-imidazooxazole derivative with promising action against tuberculosis *in vitro* and in mice, *PLoS Med*, 3 (2006) e466.
- [6] A.H. Diacon, R. Dawson, F. von Groote-Bidlingmaier, G. Symons, A. Venter, P.R. Donald, C. van Niekerk, D. Everitt, H. Winter, P. Becker, C.M. Mendel, M.K. Spigelman, 14-day bactericidal activity of PA-824, bedaquiline, pyrazinamide, and moxifloxacin combinations: a randomised trial, *Lancet*, 380 (2012) 986-993.
- [7] A.A. Velayati, M.R. Masjedi, P. Farnia, P. Tabarsi, J. Ghanavi, A.H. Ziazarifi, S.E. Hoffner, Emergence of new forms of totally drug-resistant tuberculosis bacilli: super extensively drug-resistant tuberculosis or totally drug-resistant strains in iran, *Chest*, 136 (2009) 420-425.
- [8] C.D. Acosta, A. Dadu, A. Ramsay, M. Dara, Drug-resistant tuberculosis in Eastern Europe: challenges and ways forward, *Public Health Action*, 4 (2014) S3-S12.
- [9] G. Gunther, Multidrug-resistant and extensively drug-resistant tuberculosis: a review of current concepts and future challenges, *Clinical medicine*, 14 (2014) 279-285.

- [10] G. Gunther, F. van Leth, N. Altet, M. Dedicoat, R. Duarte, G. Gualano, H. Kunst, I. Muylle, V. Spinu, S. Tiberi, P. Viiklepp, C. Lange, Beyond multidrug-resistant tuberculosis in Europe: a TBNET study, *Int J Tuberc Lung Dis*, 19 (2015) 1524-1527.
- [11] J.A. Aeschlimann, A. Stempel. Heterocyclic antituberculous compounds. US2665279, **1954**.
- [12] A.E. Wilder Smith, The Action of Phosgene on Acid Hydrazides to Give 1, 3, 4-Oxadiazolones of Interest in the Treatment of Tuberculosis, *Science*, 119 (1954) 514.
- [13] A.E. Wilder Smith, H. Brodhage, Biological spectrum of some new tuberculostatic 1,3,4-oxadiazolones with special reference to cross-resistance and rates of emergence of resistance, *Nature*, 192 (1961) 1195.
- [14] A.E. Wilder Smith, H. Brodhage, G. Haukenes, Some tuberculostatic 1,3,4-oxadiazolones(-5) and 1,3,4-oxadiazolthiones(-5). II: Biological spectrum in vitro and activity in vivo in relation to resistance emergence, *Arzneimittel-Forschung*, 12 (1962) 275-280.
- [15] A.E. Wilder Smith, Some recently synthesised tuberculostatic 4-substituted oxadiazolones and oxadiazol-thiones. VI, *Arzneimittel-Forschung*, 16 (1966) 1034-1038.
- [16] M.G. Mamolo, D. Zampieri, L. Vio, M. Fermeiglia, M. Ferrone, S. Pricl, G. Scialino, E. Banfi, Antimycobacterial activity of new 3-substituted 5-(pyridin-4-yl)-3H-1,3,4-oxadiazol-2-one and 2-thione derivatives. Preliminary molecular modeling investigations, *Bioorg Med Chem.*, 13 (2005) 3797-3809.
- [17] D. Zampieri, M.G. Mamolo, E. Laurini, M. Fermeiglia, P. Posocco, S. Pricl, E. Banfi, G. Scialino, L. Vio, Antimycobacterial activity of new 3,5-disubstituted 1,3,4-oxadiazol-2(3H)-one derivatives. Molecular modeling investigations, *Bioorg Med Chem.*, 17 (2009) 4693-4707.
- [18] A. Bellamine, A.T. Mangla, W.D. Nes, M.R. Waterman, Characterization and catalytic properties of the sterol 14 $\alpha$ -demethylase from *Mycobacterium tuberculosis*, *Proc Natl Acad Sci USA*, 96 (1999) 8937-8942.
- [19] D.J. Sheehan, C.A. Hitchcock, C.M. Sibley, Current and emerging azole antifungal agents, *Clin Microbiol Rev.*, 12 (1999) 40-79.

- [20] K.J. McLean, A.J. Dunford, R. Neeli, M.D. Driscoll, A.W. Munro, Structure, function and drug targeting in *Mycobacterium tuberculosis* cytochrome P450 systems, *Arch Biochem Biophys.*, 464 (2007) 228-240.
- [21] Y. Ben Ali, H. Chahinian, S. Petry, G. Muller, R. Lebrun, R. Verger, F. Carrière, L. Mandrich, M. Rossi, G. Manco, L. Sarda, A. Abousalham, Use of an Inhibitor To Identify Members of the Hormone-Sensitive Lipase Family, *Biochemistry*, 45 (2006) 14183-14191.
- [22] Y. Ben Ali, R. Verger, F. Carrière, S. Petry, G. Muller, A. Abousalham, The molecular mechanism of human hormone-sensitive lipase inhibition by substituted 3-phenyl-5-alkoxy-1,3,4-oxadiazol-2-ones, *Biochimie*, 94 (2012) 137-145.
- [23] V. Delorme, S.V. Diomandé, L. Dedieu, J.-F. Cavalier, F. Carrière, L. Kremer, J. Leclaire, F. Fotiadu, S. Canaan, *MmPPOX* Inhibits *Mycobacterium tuberculosis* Lipolytic Enzymes Belonging to the Hormone-Sensitive Lipase Family and Alters Mycobacterial Growth, *PLoS ONE*, 7 (2012) e46493.
- [24] B. Borgström, Mode of action of tetrahydrolipstatin: A derivative of the naturally occurring lipase inhibitor lipstatin, *Biochim. Biophys. Acta*, 962 (1988) 308-316.
- [25] P. Hadváry, W. Sidler, W. Meister, W. Vetter, H. Wolfer, The lipase inhibitor tetrahydrolipstatin binds covalently to the putative active site serine of pancreatic lipase, *J. Biol. Chem.*, 266 (1991) 2021-2027.
- [26] A. Bénarouche, V. Point, F. Carrière, J.-F. Cavalier, Using the reversible inhibition of gastric lipase by Orlistat for investigating simultaneously lipase adsorption and substrate hydrolysis at the lipid-water interface, *Biochimie*, 101 (2014) 221-231.
- [27] V. Point, A. Bénarouche, J. Zarillo, A. Guy, R. Magnez, L. Fonseca, B. Raux, J. Leclaire, G. Buono, F. Fotiadu, T. Durand, F. Carrière, C. Vaysse, L. Couédelo, J.-F. Cavalier, Slowing down fat digestion and absorption by an oxadiazolone inhibitor targeting selectively gastric lipolysis, *Eur. J. Med. Chem.*, 123 (2016) 834-848.

- [28] V.K. Sambandamurthy, S.C. Derrick, T. Hsu, B. Chen, M.H. Larsen, K.V. Jalapathy, M. Chen, J. Kim, S.A. Porcelli, J. Chan, S.L. Morris, W.R. Jacobs, Jr., Mycobacterium tuberculosis DeltaRD1 DeltapanCD: a safe and limited replicating mutant strain that protects immunocompetent and immunocompromised mice against experimental tuberculosis, *Vaccine*, 24 (2006) 6309-6320.
- [29] J.C. Palomino, A. Martin, M. Camacho, H. Guerra, J. Swings, F. Portaels, Resazurin microtiter assay plate: simple and inexpensive method for detection of drug resistance in Mycobacterium tuberculosis, *Antimicrob Agents Chemother*, 46 (2002) 2720-2722.
- [30] J. Rybniker, A. Vocat, C. Sala, P. Busso, F. Pojer, A. Benjak, S.T. Cole, Lansoprazole is an antituberculous prodrug targeting cytochrome bc1, *Nat. Commun.*, 6 (2015) 7659.
- [31] P.C. Nguyen, V. Delorme, A. Bénarouche, B.P. Martin, R. Paudel, G.R. Gnawali, A. Madani, R. Puppo, V. Landry, L. Kremer, P. Brodin, C.D. Spilling, J.-F. Cavalier, S. Canaan, Cyclipostins and Cyclophostin analogs as promising compounds in the fight against tuberculosis, *Scientific Reports*, 7 (2017) 11751.
- [32] P.C. Nguyen, A. Madani, P. Santucci, B.P. Martin, R.R. Paudel, S. Delattre, J.-L. Herrmann, C.D. Spilling, L. Kremer, S. Canaan, J.-F. Cavalier, Cyclophostin and Cyclipostins analogs, new promising molecules to treat mycobacterial-related diseases, *Int J Antimicrob. Agents*, 51 (2018) 651-654.
- [33] R.J. Wallace, Jr., D.R. Nash, L.C. Steele, V. Steingrube, Susceptibility testing of slowly growing mycobacteria by a microdilution MIC method with 7H9 broth, *J Clin Microbiol*, 24 (1986) 976-981.
- [34] A. Aubry, V. Jarlier, S. Escolano, C. Truffot-Pernot, E. Cambau, Antibiotic susceptibility pattern of Mycobacterium marinum, *Antimicrob Agents Chemother*, 44 (2000) 3133-3136.
- [35] N. Ritz, M. Tebruegge, T.G. Connell, A. Sievers, R. Robins-Browne, N. Curtis, Susceptibility of Mycobacterium bovis BCG vaccine strains to antituberculous antibiotics, *Antimicrob Agents Chemother*, 53 (2009) 316-318.

- [36] T. Christophe, M. Jackson, H.K. Jeon, D. Fenistein, M. Contreras-Dominguez, J. Kim, A. Genovesio, J.P. Carralot, F. Ewann, E.H. Kim, S.Y. Lee, S. Kang, M.J. Seo, E.J. Park, H. Skovierova, H. Pham, G. Riccardi, J.Y. Nam, L. Marsollier, M. Kempf, M.L. Joly-Guillou, T. Oh, W.K. Shin, Z. No, U. Nehrbass, R. Brosch, S.T. Cole, P. Brodin, High content screening identifies decaprenyl-phosphoribose 2' epimerase as a target for intracellular antimycobacterial inhibitors, *PLoS Pathog*, 5 (2009) e1000645.
- [37] T. Christophe, F. Ewann, H.K. Jeon, J. Cechetto, P. Brodin, High-content imaging of *Mycobacterium tuberculosis*-infected macrophages: an in vitro model for tuberculosis drug discovery, *Future Med. Chem.*, 2 (2010) 1283-1293.
- [38] P. Brodin, T. Christophe, High-content screening in infectious diseases, *Curr Opin Chem Biol*, 15 (2011) 534-539.
- [39] M. Flipo, M. Desroses, N. Lecat-Guillet, B. Dirie, X. Carette, F. Leroux, C. Piveteau, F. Demirkaya, Z. Lens, P. Rucktooa, V. Villeret, T. Christophe, H.K. Jeon, C. Locht, P. Brodin, B. Deprez, A.R. Baulard, N. Willand, Ethionamide boosters: synthesis, biological activity, and structure-activity relationships of a series of 1,2,4-oxadiazole EthR inhibitors, *J Med Chem.*, 54 (2011) 2994-3010.
- [40] J. Neres, R.C. Hartkoorn, L.R. Chiarelli, R. Gadupudi, M.R. Pasca, G. Mori, A. Venturelli, S. Savina, V. Makarov, G.S. Kolly, E. Molteni, C. Binda, N. Dhar, S. Ferrari, P. Brodin, V. Delorme, V. Landry, A.L. de Jesus Lopes Ribeiro, D. Farina, P. Saxena, F. Pojer, A. Carta, R. Luciani, A. Porta, G. Zanoni, E. De Rossi, M.P. Costi, G. Riccardi, S.T. Cole, 2-Carboxyquinoxalines Kill *Mycobacterium tuberculosis* through Noncovalent Inhibition of DprE1, *ACS Chemical Biology*, 10 (2015) 705-714.
- [41] M.S. Ravindran, S.P. Rao, X. Cheng, A. Shukla, A. Cazenave-Gassiot, S.Q. Yao, M.R. Wenk, Targeting Lipid Esterases in *Mycobacteria* Grown Under Different Physiological Conditions Using Activity-based Profiling with Tetrahydrolipstatin (THL), *Molecular & Cellular Proteomics*, 13 (2014) 435-448.

- [42] J. Lehmann, J. Vomacka, K. Esser, M. Nodwell, K. Kolbe, P. Ramer, U. Protzer, N. Reiling, S.A. Sieber, Human lysosomal acid lipase inhibitor lalistat impairs *Mycobacterium tuberculosis* growth by targeting bacterial hydrolases, *MedChemComm*, 7 (2016) 1797-1801.
- [43] C. Ortega, L.N. Anderson, A. Frando, N.C. Sadler, R.W. Brown, R.D. Smith, A.T. Wright, C. Grundner, Systematic Survey of Serine Hydrolase Activity in *Mycobacterium tuberculosis* Defines Changes Associated with Persistence, *Cell Chem Biol*, 23 (2016) 290-298.
- [44] K.R. Tallman, S.R. Levine, K.E. Beatty, Small Molecule Probes Reveal Esterases with Persistent Activity in Dormant and Reactivating *Mycobacterium tuberculosis*, *ACS Infect. Dis.*, 2 (2016) 936-944.
- [45] S. Canaan, D. Maurin, H. Chahinian, B. Pouilly, C. Dourousseau, F. Frassinetti, L. Scappuccini-Calvo, C. Cambillau, Y. Bourne, Expression and characterization of the protein Rv1399c from *Mycobacterium tuberculosis*. A novel carboxyl esterase structurally related to the HSL family, *Eur J Biochem*, 271 (2004) 3953-3961.
- [46] G. Singh, S. Arya, D. Narang, D. Jadeja, U.D. Gupta, K. Singh, J. Kaur, Characterization of an acid inducible lipase Rv3203 from *Mycobacterium tuberculosis* H37Rv, *Mol Biol Rep*, 41 (2014) 285-296.
- [47] N.P. West, F.M. Chow, E.J. Randall, J. Wu, J. Chen, J.M. Ribeiro, W.J. Britton, Cutinase-like proteins of *Mycobacterium tuberculosis*: characterization of their variable enzymatic functions and active site identification, *FASEB J.*, 23 (2009) 1694-1704.
- [48] K. Côtes, R. Dhouib, I. Douchet, H. Chahinian, A. De Caro, F. Carriere, S. Canaan, Characterization of an exported monoglyceride lipase from *Mycobacterium tuberculosis* possibly involved in the metabolism of host cell membrane lipids, *Biochem J.*, 408 (2007) 417-427.
- [49] J.C. Sacchettini, D.R. Ronning, The mycobacterial antigens 85 complex--from structure to function: response, *Trends Microbiol*, 8 (2000) 441.
- [50] J.T. Belisle, V.D. Vissa, T. Sievert, K. Takayama, P.J. Brennan, G.S. Besra, Role of the major antigen of *Mycobacterium tuberculosis* in cell wall biogenesis, *Science*, 276 (1997) 1420-1422.

- [51] L. Alibaud, Y. Rombouts, X. Trivelli, A. Burguiere, S.L. Cirillo, J.D. Cirillo, J.F. Dubremetz, Y. Guerardel, G. Lutfalla, L. Kremer, A Mycobacterium marinum TesA mutant defective for major cell wall-associated lipids is highly attenuated in Dictyostelium discoideum and zebrafish embryos, *Molecular Microbiology*, 80 (2011) 919-934.
- [52] S. Lun, W.R. Bishai, Characterization of a Novel Cell Wall-anchored Protein with Carboxylesterase Activity Required for Virulence in Mycobacterium tuberculosis, *J Biol Chem.*, 282 (2007) 18348-18356.
- [53] R.A. Slayden, C.E. Barry, 3rd, The role of KasA and KasB in the biosynthesis of meromycolic acids and isoniazid resistance in Mycobacterium tuberculosis, *Tuberculosis (Edinb)*, 82 (2002) 149-160.
- [54] G. Johnson, The alpha/beta Hydrolase Fold Proteins of Mycobacterium tuberculosis, With Reference to their Contribution to Virulence, *Curr Protein Pept Sci*, 18 (2017) 190-210.
- [55] M. Schué, D. Maurin, R. Dhouib, J.C. Bakala N'Goma, V. Delorme, G. Lambeau, F. Carriere, S. Canaan, Two cutinase-like proteins secreted by Mycobacterium tuberculosis show very different lipolytic activities reflecting their physiological function, *Faseb J*, 24 (2010) 1893-1903.
- [56] P.C. Nguyen, V.S. Nguyen, B.P. Martin, P. Fourquet, L. Camoin, C.D. Spilling, J.-F. Cavalier, C. Cambillau, S. Canaan, Biochemical and structural characterization of TesA, a major thioesterase required for outer-envelope lipid biosynthesis in M. tuberculosis, *J. Mol. Biol.*, under revision (2018).
- [57] V. Point, R.K. Malla, S. Diomande, B.P. Martin, V. Delorme, F. Carriere, S. Canaan, N.P. Rath, C.D. Spilling, J.-F. Cavalier, Synthesis and kinetic evaluation of Cyclophostin and Cyclophostins phosphonate analogs as selective and potent inhibitors of microbial lipases, *J Med Chem.*, 55 (2012) 10204-10219.
- [58] C. Rens, F. Laval, M. Daffe, O. Denis, R. Frita, A. Baulard, R. Wattiez, P. Lefevre, V. Fontaine, Effects of lipid-lowering drugs on vancomycin susceptibility of mycobacteria, *Antimicrobial Agents and Chemotherapy*, 60 (2016) 6193-6199.

- [59] B. Brust, M. Lecoufle, E. Tuailon, L. Dedieu, S. Canaan, V. Valverde, L. Kremer, Mycobacterium tuberculosis Lipolytic Enzymes as Potential Biomarkers for the Diagnosis of Active Tuberculosis, PLoS One, 6 (2011) e25078.
- [60] L. Dedieu, C. Serveau-Avesque, L. Kremer, S. Canaan, Mycobacterial lipolytic enzymes: A gold mine for tuberculosis research, Biochimie, 95 (2013) 66-73.
- [61] C. Deb, J. Daniel, T. Sirakova, B. Abomoelak, V. Dubey, P. Kolattukudy, A Novel Lipase Belonging to the Hormone-sensitive Lipase Family Induced under Starvation to Utilize Stored Triacylglycerol in Mycobacterium tuberculosis, J. Biol. Chem., 281 (2006) 3866-3875.
- [62] R. Dhouib, A. Ducret, P. Hubert, F. Carriere, S. Dukan, S. Canaan, Watching intracellular lipolysis in mycobacteria using time lapse fluorescence microscopy, Biochim Biophys Acta, 1811 (2011) 234-241.
- [63] O. Neyrolles, R. Hernández-Pando, F. Pietri-Rouxel, P. Fornès, L. Tailleux, J.A. Payán, E. Pivert, Y. Bordat, D. Aguilar, M.C. Prévost, Is Adipose Tissue a Place for Mycobacterium tuberculosis Persistence?, PLoS ONE, 1 (2006) e43.
- [64] P. Peyron, J. Vaubourgeix, Y. Poquet, F. Levillain, C. Botanch, F. Bardou, M. Daffe, J.F. Emile, B. Marchou, P.J. Cardona, C. de Chastellier, F. Altare, Foamy macrophages from tuberculous patients' granulomas constitute a nutrient-rich reservoir for M. tuberculosis persistence, PLoS Pathog, 4 (2008) e1000204.
- [65] P. Santucci, F. Bouzid, N. Smichi, I. Poncin, L. Kremer, C. De Chastellier, M. Drancourt, S. Canaan, Experimental Models of Foamy Macrophages and Approaches for Dissecting the Mechanisms of Lipid Accumulation and Consumption during Dormancy and Reactivation of Tuberculosis, Front Cell Infect Microbiol, 6 (2016) 122.
- [66] P. Santucci, S. Diomandé, I. Poncin, L. Alibaud, A. Viljoen, L. Kremer, C. de Chastellier, S. Canaan, Delineating the physiological roles of the PE and catalytic domain of LipY in lipid consumption in mycobacteria-infected foamy macrophages, Infect Immun., (2018) DOI: 10.1128/iai.00394-00318.

- [67] V. Point, K.V.P. Pavan Kumar, S. Marc, V. Delorme, G. Parsiegla, S. Amara, F. Carrière, G. Buono, F. Fotiadu, S. Canaan, J. Leclaire, J.-F. Cavalier, Analysis of the discriminative inhibition of mammalian digestive lipases by 3-phenyl substituted 1,3,4-oxadiazol-2(3*H*)-ones, *European Journal of Medicinal Chemistry*, 58 (2012) 452-463.
- [68] K. Pethe, P. Bifani, J. Jang, S. Kang, S. Park, S. Ahn, J. Jiricek, J. Jung, H.K. Jeon, J. Cechetto, T. Christophe, H. Lee, M. Kempf, M. Jackson, A.J. Lenaerts, H. Pham, V. Jones, M.J. Seo, Y.M. Kim, M. Seo, J.J. Seo, D. Park, Y. Ko, I. Choi, R. Kim, S.Y. Kim, S. Lim, S.-A. Yim, J. Nam, H. Kang, H. Kwon, C.-T. Oh, Y. Cho, Y. Jang, J. Kim, A. Chua, B.H. Tan, M.B. Nanjundappa, S.P.S. Rao, W.S. Barnes, R. Wintjens, J.R. Walker, S. Alonso, S. Lee, J. Kim, S. Oh, T. Oh, U. Nehrbass, S.-J. Han, Z. No, J. Lee, P. Brodin, S.-N. Cho, K. Nam, J. Kim, Discovery of Q203, a potent clinical candidate for the treatment of tuberculosis, *Nat Med*, 19 (2013) 1157-1160.
- [69] A. Shevchenko, M. Wilm, O. Vorm, M. Mann, Mass spectrometric sequencing of proteins silver-stained polyacrylamide gels, *Anal Chem.*, 68 (1996) 850-858.
- [70] J. Cox, M. Mann, MaxQuant enables high peptide identification rates, individualized p.p.b.-range mass accuracies and proteome-wide protein quantification, *Nat Biotechnol.*, 26 (2008) 1367-1372.
- [71] J.A. Vizcaino, E.W. Deutsch, R. Wang, A. Csordas, F. Reisinger, D. Rios, J.A. Dienes, Z. Sun, T. Farrah, N. Bandeira, P.A. Binz, I. Xenarios, M. Eisenacher, G. Mayer, L. Gatto, A. Campos, R.J. Chalkley, H.J. Kraus, J.P. Albar, S. Martinez-Bartolome, R. Apweiler, G.S. Omenn, L. Martens, A.R. Jones, H. Hermjakob, ProteomeXchange provides globally coordinated proteomics data submission and dissemination, *Nat Biotechnol.*, 32 (2014) 223-226.
- [72] A. Viljoen, M. Richard, P.C. Nguyen, P. Fourquet, L. Camoin, R.R. Paudal, G.R. Gnawali, C.D. Spilling, J.-F. Cavalier, S. Canaan, M. Blaise, L. Kremer, Cyclopostins and Cyclophostin analogs inhibit the antigen 85C from *Mycobacterium tuberculosis* both *in vitro* and *in vivo*, *J. Biol. Chem.*, 293 (2018) 2755-2769.

**Highlights**

The OX analogs represent a novel class of multi-target inhibitors against *M. tb*

Some OX inhibit either extracellular, or both intra- and extracellular *M. tb* growth

These OXs are not toxic towards host macrophages

OX probes are attractive chemical tools to identify (Ser/Cys)-enzymes in living mycobacteria

## Graphical abstract

